STUDIES ON

THE ELECTRONIC FACTOR

IN CATALYSIS

Thesis presented for the degree of Doctor of Philosophy

by

David F. Quinn

University of Edinburgh

September 1962

PREFACE

This thesis is concerned with a study of the decomposition of formic acid, and of methanol, on alloy catalysts of copper and nickel with particular reference to the electronic factor in catalysis.

ABSTRACT OF THESIS

Name of Candidate David Forbes Quinn

Address _____

Degree Doctor of Philosophy *Date* September 1962.

Title of Thesis Studies on the Electronic Factor in Catalysis

Metals which possess vacant electronic energy states in the d-band should, according to the electronic factor theory, be efficient catalysts for processes involving the formation of essentially covalently bound chemisorbed species. Nickel is such a metal.

By alloying nickel with copper, a continuous series of solid solutions are obtained. In doing so, the 'geometric' structure of these alloys does not change to any great extent with variation in composition, but pronounced changes in electronic structure occur. According to the theory, the number of holes in the d-band should be zero for all alloys of copper content greater than 60 atom percent. Thus for reactions involving a complex of the above type, there should be a change in activity of catalysts near this composition.

A series of copper-nickel alloy catalysts were prepared chemically from their mixed carbonates. Both constituents were analysed independently. The surface area of the alloys was measured by argon adsorption at -196 °C. X-ray diffraction and magnetic susceptibility measurements were carried out on the alloys, and from these results, and by comparison with those in the literature, it seems that the catalysts used were homogeneous solid solutions. The magnetic susceptibility results, however, indicate the presence of d-band vacancies at copper contents as high as 90 atom percent copper. This is in agreement with other results in the literature, and it seems that for the copper-nickel system, any change in activity pattern which is to be observed from an electronic effect will not become apparent until very high copper contents are reached.

Two 'test' reactions, which are catalysed by many metals and alloys, were used in this study. They were the decomposition of formic acid and the decomposition of methanol. In both cases there is only one reactant and the reaction can be followed easily by pressure measurements. A static system was used. The decomposition of formic acid was carried out between 80 and 200 °C at pressures up to 28 mm. Hg.

Use other side if necessary.

/ and the methanol decomposition from 140 to 330 °C at pressures of approximately 12 and 25 mm. Hg on eight alloys of copper and nickel and on the pure metals.

Previous work using both reactions on various alloys has given support to the electronic factor theory, but recently the role of the electronic factor in the decomposition of formic acid has been strongly criticised. The theory has been put forward that the decomposition takes place via the formation of an intermediate metal formate film, and the activity of a metal has been related to the heat of formation of its formate. Accordingly, copper is claimed to be more active than nickel for the formic acid decomposition.

The results of the present work for this decomposition show an activity pattern in keeping with the electronic factor theory, a decrease in activity being apparent at high copper contents. A similar but more pronounced pattern was obtained for the methanol decomposition. It therefore seems likely that both these decompositions are controlled by a similar electronic factor, and that the formic acid decomposition probably takes place via the formation of a covalently bound complex of the 'formate' type, but that it does not involve the transfer of an electron from the catalyst to the adsorbent as required by the metal formate film mechanism.

ACKNOWLEDGEMENTS

I should like to thank my supervisor, Dr. Duncan Taylor, for his guidance and encouragement during the course of this work.

I am also indebted to Professor T.L. Cotterell for the interest he has shown in this work, and to him and Professor E.L. Hirst for the provision of laboratory facilities.

I am grateful to Dr. C. Beevers and Dr. D. Anderson for the use of the diffractometer and the spectrophotometer respectively, and to Mr. Musgrave for experiments with the flow system.

Acknowledgement is made for the award of a Research Studentship from the Department of Scientific and Industrial Research.

CONTENTS

INTRODUCTION

In heteregeneous catalysis involving a solid catalyst and gaseous reactants, it is necessary that at least one of the reactants be chemisorbed onto the surface of the catalyst to form some type of activated complex which may then undergo further stages of reaction. The catalytic effect of the adsorbent can, in very general terms, be considered in the light of two factors. One of these, the 'geometric factor', relates catalytic activity to crystal structure and cell dimensions and makes several important assumptions[1]. The other, the 'electronic factor'[2,3], takes into account the part the electronic structure of the solid plays in catalysis.

Therefore to study the electronic factor in catalysis it is desirable to keep the geometric structure of the catalyst as constant as possible while the composition is varied in such a manner as to cause pronounced changes in the electronic factor. In this way the results obtained will be almost entirely dependent on the electronic structure of the catalyst.

The transition metals have long been recognised as catalysts for many reactions and a rough correlation between their specific activity and position in the Periodic Table has been observed[1,4]. In recent years however the 'electronic factor' concept in catalysis has come into prominance as one of the more sucessful hypotheses in explaining the catalytic activity of solids and of the transition metals in particular.

The 'electronic factor' theory suggests that the activity of a metal will depend on the extent to which the metal d-band (which in the bulk metal replaces the atomic d-orbitals[5]) is occupied.

Thus transition metals possessing a number of vacant electronic energy states in the d - band should, according to the theory, be efficient catalysts for processes involving the formation of essentially covalently bound chemisorbed species, or of species which, as a result of some type of electron transfer process during chemisorption, tend to become charged.

If the formation of such chemisorbed species is the rate determining stage in a reaction, then the activity of a series of 'geometrically' similar catalysts should decrease as the concentration of vacancies in the d - band decreases [1].

The outermost electrons of the transition metals are considered by Mott and Jones [6] to occupy two bands. In the case of nickel, the ten outermost electrons per atom are shared between the overlapping 3d and 4s-bands. From the saturation magnetization intensity expressed in Bohr magnetons per atom the average number of holes in the d - band of nickel is shown to be 0.6, that is an average of 9.4 electrons per atom in the d - band.

By alloying copper with nickel a continuous series of solid solutions are obtained, the nickel atoms in the lattice being replaced by copper [7]. Since copper has a theoretically completely filled 3d - band, extra electrons will be added to the lattice. These added electrons will initially enter the d - band since the density of states there, is much greater than in the s - band.

The saturation magnetic moment of these alloys decreases as the atom percentage of copper increases. On extrapolation to zero magnetic moment it is seen that, to a first approximation, the number of holes in the d - band will be reduced to zero for an alloy containing 60 atom percent copper [6].

At this point there should be a fundemental change in the electronic structure of the solid solution. Thus there should be a gradual decrease in specific activity of catalysts as the copper content increases from 0 to 60 atom percent, or there may be quite a sudden change in activity near the critical composition.

The various possible idealised forms of activity pattern predicted by this theory for the dependence of activity on composition for alloys of copper and nickel have been given by Bond and Mann [8].

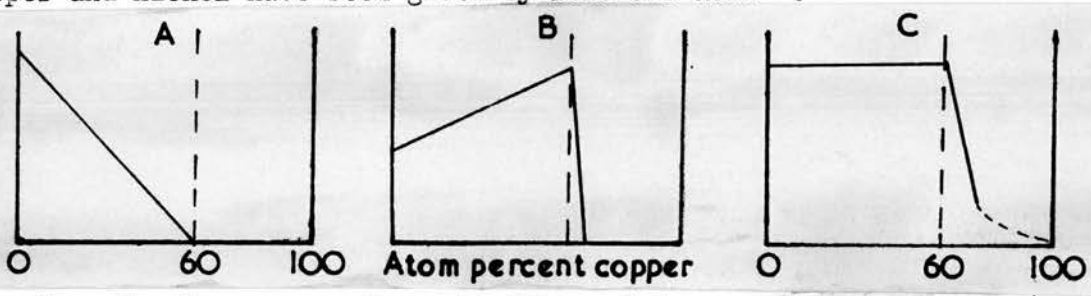

In order to compare the activities of these catalysts in gas / solid interface processes, a simple and reproducible test reaction can be used. Hydrogenation and dehydrogenation reactions have been used extensively as test reactions for catalysis by metals.

The results of Bond and Mann [8] for hydrogenation of acetylene showed all three activity patterns, the prevailing pattern being dependent on the temperature at which the reaction was carried out.

For the hydrogenation of styrene Dowden and Reynolds [9] obtained results similar to that shown in figure A, namely a gradual decrease in activity as the d - band is filled with little or no activity when the band is completely filled. The results of Hall and Emmett [10] for the hydrogenation of ethylene over copper - nickel alloys show a similar pattern when plotted as rate against /

/ composition but an increase in activation energy is observed for the pure metals.

In figure B the idealised pattern is that to be expected when there is a continuous decrease in the strengths of adsorption as the d-band is filled. The ethylene hydrogenation results of Best and Russell [11] conform to this pattern, and also in a very general sense, the results of Hall and Emmett [12] for the hydrogenation of benzene.

The activity - composition pattern C results when the rate controlling factor is the density of occupied electronic states in the d-band the rate being independent of the concentration of vacancies as long as any are present. Such a pattern was obtained by Rienacker and Bommer [13] for the hydrogenation of ethylene over copper - nickel alloys at high temperatures. Recently Tuul and Farnsworth [14] using the same reaction and the same alloys found a sudden decrease in activity for pure copper, a decrease which they did not relate to the electronic factor interpretation, but which according to Dowden's theory [1] could conform to the pattern in figure C.

Since hydrogenation reactions involve two molecular species (which increases the number of possible mechanisms), dehydrogenation reactions have an advantage in investigations of the electronic factor in catalysis.

The decomposition of formic acid or methanol vapours provide such reactions.

$$H\,COOH \longrightarrow CO + H_2O$$

$$H\,COOH \longrightarrow CO_2 + H_2$$

$$CH_3OH \longrightarrow CO + 2H_2$$

There is only one reactant, the rate can be followed easily by pressure measurements, and the decompositions are catalysed by many metals and alloys.

Previous work on the formic acid reaction by Dowden and Reynolds [9] and to a lesser extent by Rienacker [15], on alloys of copper and nickel support the electronic factor interpretation. Dowden found a decrease in activity very similar to that given in figure A, and Rienacker noted a large increase in activation energy for alloys with 0 - 20 atom percent nickel. This was associated with a peak in the activity pattern at 20 atom percent nickel. The results of Luetic and Brihta [16] for copper - nickel alloys supported on alumina are similar in activation energy pattern to those of Rienacker but with an even larger variation. Schwab [17] in a limited investigation of this system using foils found no variation in activation energy with composition.

Eley and Luetic [18], and Schwab [19], found, for the palladium - gold and palladium - silver systems respectively, an increase in activation energy as the Brillouin zone approaches a saturation limit, which results again agree generally with the electronic factor concept.

On the other hand, Fahrenfort and his Dutch school [20,21]. have taken the view that in the formic acid reaction the electronic factor is unimportant. This they conclude from infra - red absorption measurements. Strong absorption bands at 1360 and 1575 cm^{-1} were observed on nickel when formic acid was chemisorbed onto it. Since the infra - red spectra of metal formates gives bands of similar wave lengths which are generally ascribed to the formate ion, they consider the reaction takes place via the formation and decomposition of a metal formate film. Hirota et al [22] and Tamaru [23] have also concluded that during reaction the surface of the metal is covered by a superficial layer of formate.

The Dutch workers have related activity to the heat of formation of the metal formate for a series of pure metal catalysts. They have not investigated copper - nickel alloys, but in their view, copper and nickel do not differ greatly in activity. They claim that the adsorbate attracts electrons from the metal and becomes negatively charged and that there is no question of an electron transfer towards the catalysing metal.

It should however be pointed out that these results are in direct conflict with those Suhrmann and Wedler [24] who found a decrease of resistance of nickel films on adsorption of formic acid at low temperatures indicating an electron transfer to the catalyst.

Ruka et al [25] detected formate films but claimed they played no part in the decomposition.

As a result of these conflicting views, the decomposition of formic acid on copper and nickel and their alloys was undertaken in the hope that a decision might be reached confirming, either the metal formate film or electronic factor interpretation of the mechanism or a reconciliation of both.

In contrast to the catalytic decomposition of formic acid, the decomposition of methanol on metals has recieved only limited attention as a test reaction.

Dowden and Reynolds [9] investigated the decomposition over a series of alloys of copper and nickel and found that alloys containing more than fifty atom percent copper were less active than those with high nickel content.

Unfortunately this study was limited to only four alloys and the pure metals all of which were of small area. The results, although not very extensive do give support to the electronic factor theory.

Other work on this catalytic decomposition has not been directed towards substantiating the electronic factor theory but the mechanism suggested by Constable [26] and Balandin and Teteni [27] indicate that a change in specific activity might be observed for metals of differing d - band structure.

Since the decomposition of methanol seems less likely to involve the formation of a metal complex with the catalyst than formic acid, the decomposition was undertaken using the same alloys as for the formic acid decomposition. In this way it was hoped that any dependency on d - band vacancies, which in the formic acid decomposition might be obscured by the formation of an intermediate formate would be accentuated in the methanol decomposition.

EXPERIMENTAL

Preparation of the Copper - Nickel Alloy Catalysts.

There are several methods of preparing copper - nickel alloys, one being the fusion of the pure metals together in definite proportions in an inert atmosphere. This method has the advantage in that analysis of the alloys is unnecessary, but the surface area per gram of alloy is very small, an obvious disadvantage in heterogenous catalysis. Supported catalysts and those prepared by dissolving out a third metal may add complicating factors to the catalysis. Evaporation in vacuo provides a good method for the preparation of pure metal catalysts of moderate surface area, but evaporation methods are difficult where alloys are concerned, although recently Emmett and Gharpurey [28] have achieved this successfully. The method chosen was that given by Best and Russell [11] which is a modification of the method of Long, Fraser and Ott [29].

The preparation is reported by Hall and Alexander [30] to provide catalysts in the form of homogenous solid solutions of high purity. It also has the advantage that it does not involve heating the metals above their Tamman temperatures and so enables adequate surface areas per gram to be obtained. Furthermore, comparison of the results with related work in the literature will be facilitated since catalysts prepared in a similar way have been used by Bond and Mann [8], and Emmett [10,12], and others for investigation of the electronic factor in hydrogenation reactions.

Calculated amounts of 'Analar' $Cu(NO_3)_2.3H_2O$ and / or $Ni(NO_3)_2.6H_2O$ were dissolved in distilled water and the solutions diluted to correspond to approximately 5g NiO and / or CuO per 100ml. Reagent grade ammonium bicarbonate was added to the rapidly stirred solutions at room temperature until a faint but permanent turbidity formed. 2.2 moles of the bicarbonate per mole of metal ion(s) was then added fairly rapidly. The mixture was stirred for fifteen minutes and the precipitate then allowed to settle overnight. The precipitates were washed by decantation with hot water so that most of the nitrate ion was removed. Excess water was removed by evaporation on a steam bath and the solid dried in an oven at 105 ^{o}C for 24 hours. The basic carbonates were then heated for 4 hours at 400 ^{o}C. A portion of the resulting mixed oxides was reduced in situ in the Pyrex reaction vessel in a stream of purified electrolytic hydrogen at a flow rate of 15 ml. per minute for 24 hours, the temperature rising to 500 ^{o}C from room temperature in the first four hours. The catalyst was then allowed to cool to 20 ^{o}C, when the hydrogen was replaced by 'spot' nitrogen and the exit from the reaction vessel sealed off. The reaction vessel was then evacuated.

The catalysts were stored in their oxide form until required for the formic acid decomposition, after which they were kept under vacuum until used for the decomposition of methanol.

If at any time the alloys had to be exposed to the air, they were reduced under one atmosphere of hydrogen for 16 hours at 400 ^{o}C before reuse.

Generation and Purification of Hydrogen.

FIGURE 1

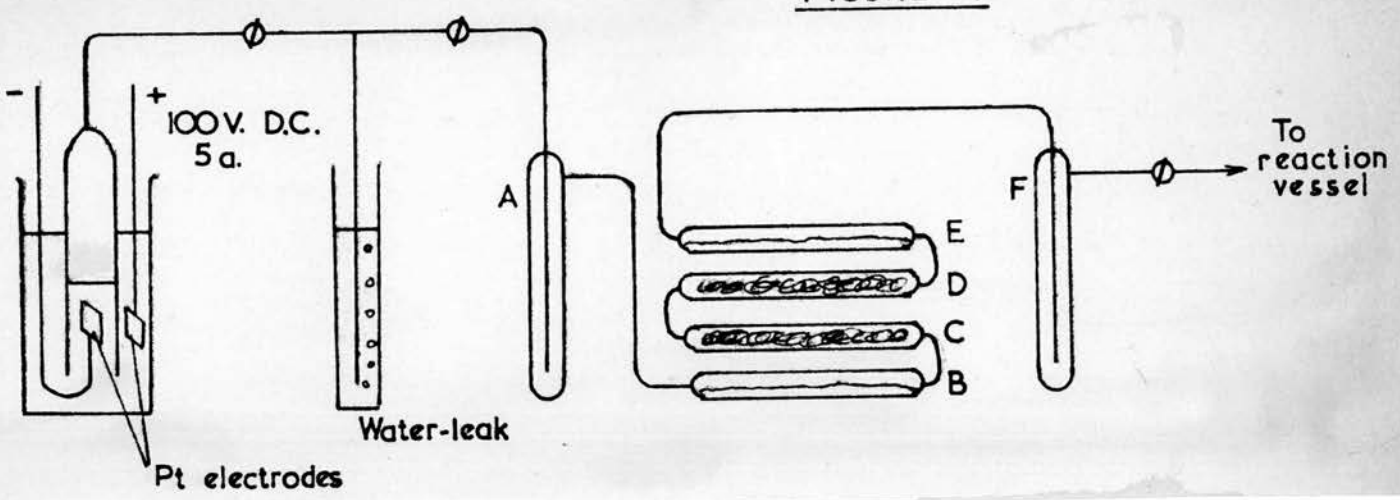

Hydrogen was generated electrolytically from a 20 percent solution of sodium hydroxide in the above apparatus (Figure 1).

A and F were liquid nitrogen traps. The purification tubes were about twelve inches long, C and D contained palladised asbestos heated electrically to 370 °C, and B and E phosphorus pentoxide.

The purification train was evacuated then hydrogen passed through it and pumped away for ten minutes before filling it to one atmosphere. Hydrogen was then allowed to enter the reaction vessel at a flow rate of 15 ml. per minute. The water-leak ensured that the hydrogen was always generated at a pressure greater than one atmosphere so that no air would enter the system.

Analysis of the Catalysts

Analyses were carried out for both copper and nickel by weighing out a portion of the mixed oxides, dissolving in a minimum of dilute hydrochloric acid and making up to a standard volume with distilled water. Copper was determined by precipitation with salicylaldoxime, and nickel with dimethyl--glyoxime. The analytical proceedures were checked with solutions prepared from known weights of 'Analar' copper and 'Hilger spectroscopic purity' nickel.

Determination of Copper

Salicylaldoxime is a specific reagent for copper if the precipitation is carried out in acetic acid at pH 3. The reagent was prepared by dissolving 2.2 g. salicylaldehyde in 8 ml. of 95 percent alcohol and adding the solution to 1.3 g. hydroxylamine hydrochloride dissolved in 2 ml. water. The resultant mixture was added to 225 ml. water at 80 °C and allowed to cool. This reagent was not very stable and therefore was renewed every two days.

A known portion of the alloy solution, corresponding to 0.05 - 0.10 g. copper, was made up to approximately 100 ml. at room temperature and 2 $\overline{N}$ sodium hydroxide added until a slight permanent precipitate formed. This was dissolved by the addition of acetic acid to pH 3. A slight excess of the salicylaldoxime reagent was then added. The precipitated complex was filtered off on a weighed sintered glass crucible and washed with water until the washings gave no red colour with ferric chloride. It was then dried to a constant weight at 100 °C and weighed as $Cu(C_7H_5O_2N)_2$. No attempt was made to analyse the filtrate for nickel.

Determination of Nickel

A one percent solution of dimethylglyoxime in alcohol was used as the reagent for the quantitative precipitation of nickel. Known aliquots of the alloy solution were diluted to about 100 ml. and heated to 70 - 80 °C. At this temperature a slight excess of dimethylglyoxime reagent was added followed by 3 - 4 g. sodium acetate. After standing for ten minutes on a steam bath the mixture was tested for complete precipitation and then digested for one hour on a boiling water bath. The precipitate was then collected in a previously weighed sintered glass crucible, washed with hot water and dried to a constant weight at 110 °C. It was weighed as $Ni(C_4H_7O_2N_2)_2$.

The results given below are the mean of at least two determinations with a maximum error of + or - one percent.

TABLE 1 Analysis of Copper - Nickel Alloy Catalysts

Catalyst	Mixed Oxides		Alloy	
	Wt. percent Nickel	Wt. percent Copper	Atom percent Nickel	Atom percent Copper
I		-	100.0	-
II	64.7	10.3	87.0	13.0
III	59.0	16.1	79.9	20.1
IV	53.8	24.4	70.7	29.3
VI	38.0	40.5	50.4	49.6
IX	27.2	51.7	36.2	63.8
XII	22.9	55.6	30.8	69.2
XIII	13.0	64.7	17.8	82.2
XIV	5.4	72.6	7.4	92.6
XV	-		-	100.0

Surface Area Measurements

The method adopted was that given by Brunauer , Emmett and Teller [31], universally known as the B.E.T. method. Schriener and Kemball [32] have suggested that Huttig's method [33] is probably more accurate since the latter's equation holds over a greater range of relative pressure. Any advantage to be gained by use of Huttig's method would be lost when a comparison of the results of other workers, who used the B.E.T. method, is made.

The B.E.T. method is to adsorb the gases onto the previously degassed solid at or near the boiling point of the gas. Near ideal gases are generally used since they obey the B.E.T. theory in its simplest form. The B.E.T. theory assumes that several layers of gas are adsorbed onto the solid surface and leads to an expression from which the volume of gas necessary to form a single layer on the surface is readily obtained.

The volume of gas adsorbed at N.T.P. is given by -

$$V = \frac{cPV_m}{(P_o - P)\,(1 + (c - 1)P / P_o)}$$

where P = pressure of gas

P_o = vapour pressure of gas at the temperature of the adsorbent

c = constant related to the heat of adsorption

V_m = volume of gas at N.T.P. necessary to form a single layer on the surface.

From this expression it can be seen that by plotting $P / (P_o - P)V$ against P / P_o a value for V_m can be obtained. This isotherm generally holds up to a relative pressure (P / P_o) of about 0.35 . Once this value of V_m has been found, the number of molecules involved in covering the surface, and so the surface area, can be calculated. In the present work satisfactory /

FIGURE 2

Adsorption Apparatus for Surface Area Measurements

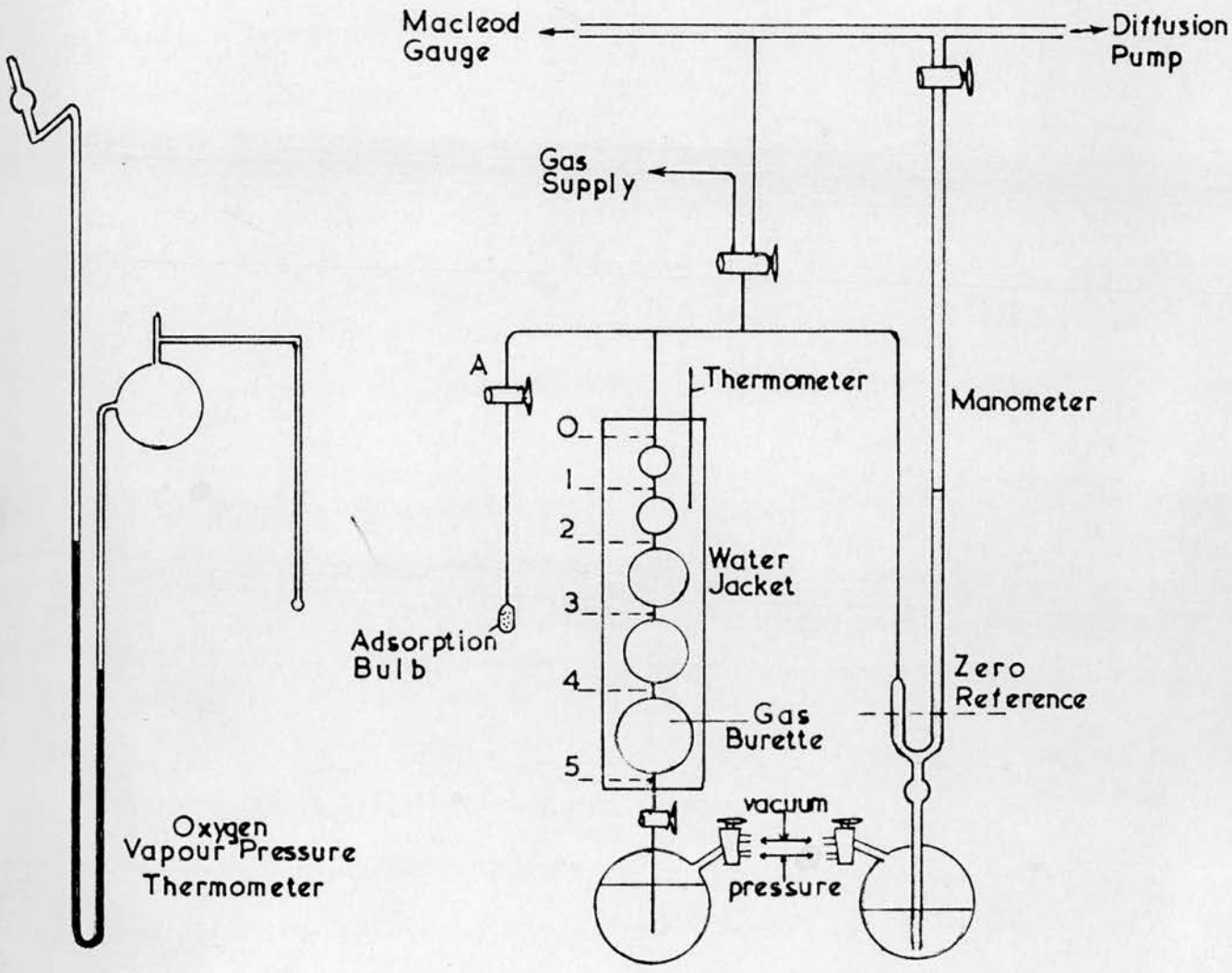

/ results were obtained using argon adsorption at - 196 °C with helium for dead space determination.

Description of Apparatus

The apparatus was as shown in Figure 2. 'Pyrex' was used throughout and 'Apiezon' L grease for all stopcocks and joints. The apparatus consisted mainly of a manometer, a gas burette for controlled increments in pressure, and the adsorption bulb containing the catalyst. Other essential components included a vapour pressure thermometer, furnace, gas reservoirs and purification train, as well as those usually associated with high vacuum systems. 2mm. bore capillary tubing was used in the adsorption system to minimise dead space.

Manometer

This was made from 10 mm. tubing to minimise meniscus effects of the mercury. This was also the diameter at the zero point in the pressure leg so that capillary effects could be avoided. The bulb below the zero point was inserted as a safety-device to avoid the mercury being forced round the U - bend if a rapid increase in pressure occurred during the manipulations. Pressure differences were measured by a vertical travelling microscope reading to + or - 0.02 mm.

Gas Burette

The burette consists of a series of five bulbs of various sizes connected by short lengths of capillary tubing having reference marks above and below each bulb. Before attaching the burette to the system the bulb volumes were accurately determined by weighing the mercury required to fill each bulb. The volumes so obtained differ by an insignificant amount from the true volumes at 0 °C. Since the burette represented the largest volume of the system, it was enclosed by a water jacket to maintain the temperature constant.

Adsorption Bulb

A bulb of about 15 mm. diameter, large enough to contain 3 - 4 g. catalyst, was blown on the end of a short length of 2 mm. bore capillary tubing. A small glass wool plug was inserted in the capillary near the bulb to prevent the catalyst being sucked out of the bulb during the degassing process.

Oxygen Vapour Pressure Thermometer

This was constructed following the directions given by Farkas and Melville [34]. It was mounted on a movable stand.

Furnace

This was a simple silica tube wound with resistance wire, a 'Sunvic' regulator being used to adjust the temperature.

Gas Reservoirs and Purification Train

The gases were stored in two-litre bulbs attached to the apparatus so that they could be evacuated and filled independently. The pressure of gas in the bulbs could be measured on the manometer. Helium, 99.8 percent purity, was further purified by passing through a liquid nitrogen trap and then a charcoal trap cooled with liquid nitrogen. Before use, the charcoal was activated by heating the trap at 105 ^{o}C for 24 hours with continuous pumping. 99.98 percent purity argon was purified in the same way, the only difference being the replacement of liquid nitrogen by liquid oxygen. The flow rate over the activated charcoal in both cases was 30 ml. per minute.

Macleod Gauge

The gauge was of standard design employing 'Veridia' capillary tubing, and was calibrated by weighing the amount of mercury required to fill the bulb and the capillary. The results were -

1. Volume of gauge bulb + capillary = 146.8 ml.
2. Volume of capillary = 0.0095 ml. per cm.

Free Volume Calibration of the Adsorption System V_o

This is the volume from stopcock A to the zero reference of the manometer with mercury at the zero mark in the gas burette. It was determined as follows.

Stopcock A was closed and the gas burette set at zero. Helium or argon was then admitted to the evacuated system to a pressure of about one atmosphere as recorded on the manometer. The mercury in the gas burette was then lowered to the No. 1 reference point and the pressure redetermined after returning the mercury to the zero reference of the manometer.

This procedure was repeated for the next reference point, and so on until all the bulbs in the gas burette had been emptied of mercury.

Since a constant amount of gas was used and the temperature was constant,

$$PV = \text{constant}$$

and $$V = V_o + V_{tB}$$

where V_{tB} is the total volume of the burette bulbs used in any given measurement.

$$\therefore \quad PV_o + PV_{tB} = \text{constant}$$

or $$PV_{tB} = \text{constant} - PV_o$$

$$\frac{d(PV_{tB})}{dP} = -V_o$$

Therefore a plot of PV_{tB} against P gives a straight line of slope $-V_o$, which is the negative of the free volume. V_o will be a volume at 0 °C since the volumes of the gas burette (V_{tB}) used, correspond to 0 °C.

Since for each reference mark on the gas burette, the volume of the system up to stopcock A ($= V_o + V_{tB}$) is now known, it is convenient to convert these volumes into volume factors (f_v) by multiplying by 273.2 / 760 .

Thus, if gas is present in the system at pressure P and temperature T, then

$$(V_o + V_{tB}) P / T = V_{N.T.P.} \; 760 / 273.2$$

and the volume of the gas at N.T.P. is given by,

$$V_{N.T.P.} = (V_o + V_{tB}) \frac{273.2}{760} \frac{P}{T} = f_V \frac{P}{T}$$

The volume factors are designated f_{Vo}, f_{V1}, f_{V2} etc., corresponding to the reference marks on the gas burette, and are constant as long as the volume of the system up to stopcock A remains unchanged.

Free Volume Calibration of the Adsorption Bulb.

This calibration must be done each time the adsorption bulb and its contents are changed.

The sample is introduced into the adsorption bulb which is then sealed onto the apparatus below stopcock A. The whole system is evacuated with the furnace at 150 °C in place round the adsorption bulb. The degassing process was continued until a pressure of 10^{-6} mm.Hg was recorded on the Macleod gauge. Stopcock A is then closed, the furnace removed and the adsorption bulb allowed to cool. The vapour pressure thermometer is placed in position beside the adsorption bulb and the two immersed in liquid nitrogen to a fixed depth. This level of liquid nitrogen is maintained throughout the surface area determination. A large sample of helium is introduced into the system with the mercury level in the gas burette set at the zero reference mark and the pressure (P) measured. From this pressure and f_{Vo} the volume of helium at N.T.P., $V_T(He)$, is calculated. Stopcock A is then opened, the new pressure, P_1, determined, and so $V_R(He)$, the volume of helium remaining in the system up to stopcock A can be calculated.

The volume of helium which entered the adsorption bulb will then be,

$$V_A(He) = V_T(He) - V_R(He) \quad \text{at N.T.P.}$$

This volume, $V_A(He)$, will be dependent on the pressure P_1 and the ratio $V_A(He) / P_1$ will be a constant since,

$$V_A(He) = f_{Vo} \frac{P}{T} - f_{Vo} \frac{P_1}{T}$$

and therefore

$$\frac{V_A(He)}{P_1} = f_{Vo} \frac{P}{P_1} \cdot \frac{1}{T} - f_{Vo} \frac{1}{T} = \text{constant}$$

This constant is the adsorption bulb factor, f_A, since its product with a given pressure will give the volume of gas at N.T.P. in the adsorption bulb.

Adsorption of Argon

The helium is pumped out of the system with the liquid nitrogen bath removed. (It is not necessary to replace the furnace since helium is not adsorbed.) After evacuation stopcock A is closed and the nitrogen bath replaced. The mercury in the gas burette is set at the No 5 reference point and a small quantity of argon admitted (i.e. enough to give a P / P_o ratio of about 0.35 at the maximum value of P). The total volume of argon at N.T.P., $V_T(A)$, is then calculated. Stopcock A is opened and after ten minutes the next pressure (P_5) is taken, this time being sufficient to allow the adsorption to reach equilibrium. The temperature of both the liquid nitrogen bath and gas burette is noted. The mercury in the gas burette is then set on point No 4 and the same proceedure carried out, P_4 being recorded this time, and so on until the gas burette has been filled with mercury.

From the pressure measurements the volume of gas adsorbed onto the surface is calculated from,

$$V_{ads} = V_T - (V_R + V_A)$$

where V_T = the total volume of gas in the system,

V_R = the volume remaining in the burette system up to stopcock A,

V_A = the volume of gas in the adsorption bulb, but not adsorbed,

all volumes being at N.T.P.

V_{ads} is calculated for each reference point on the gas burette. The vapour pressure of argon (P_o), at the temperature of the liquid nitrogen bath was obtained from 'International Critical Tables'. A plot is now made of P/P_o against $P / V_{ads}(P_o - P)$ and so a value of V_m (the volume of argon required for a monolayer) obtained, (see page 13).

Since the properties of a physically adsorbed film are more likely to be that of the liquid state, a value of 14.4 A^2 was used for the cross - sectional area of one atom of argon, this being the figure given by B.E.T. [21] for liquid argon. This figure takes into account the assumed hexagonal close packing of the atoms in the adsorbed layer. Therefore the area occupied by 1 ml. of argon at N.T.P. is equal to,

$$\frac{6.02 \cdot 10^{23} \cdot 14.4}{22,400 \cdot 10^{16} \cdot 10^{4}} = 3.88 \text{ m}^2$$

The surface area of the sample is equal to 3.88 V_m metres^2 .
The surface area quoted for each catalyst is the mean of at least three determinations, with a maximum deviation of + or - 5 percent.
The measured surface areas are shown in Table 2, on page 22.

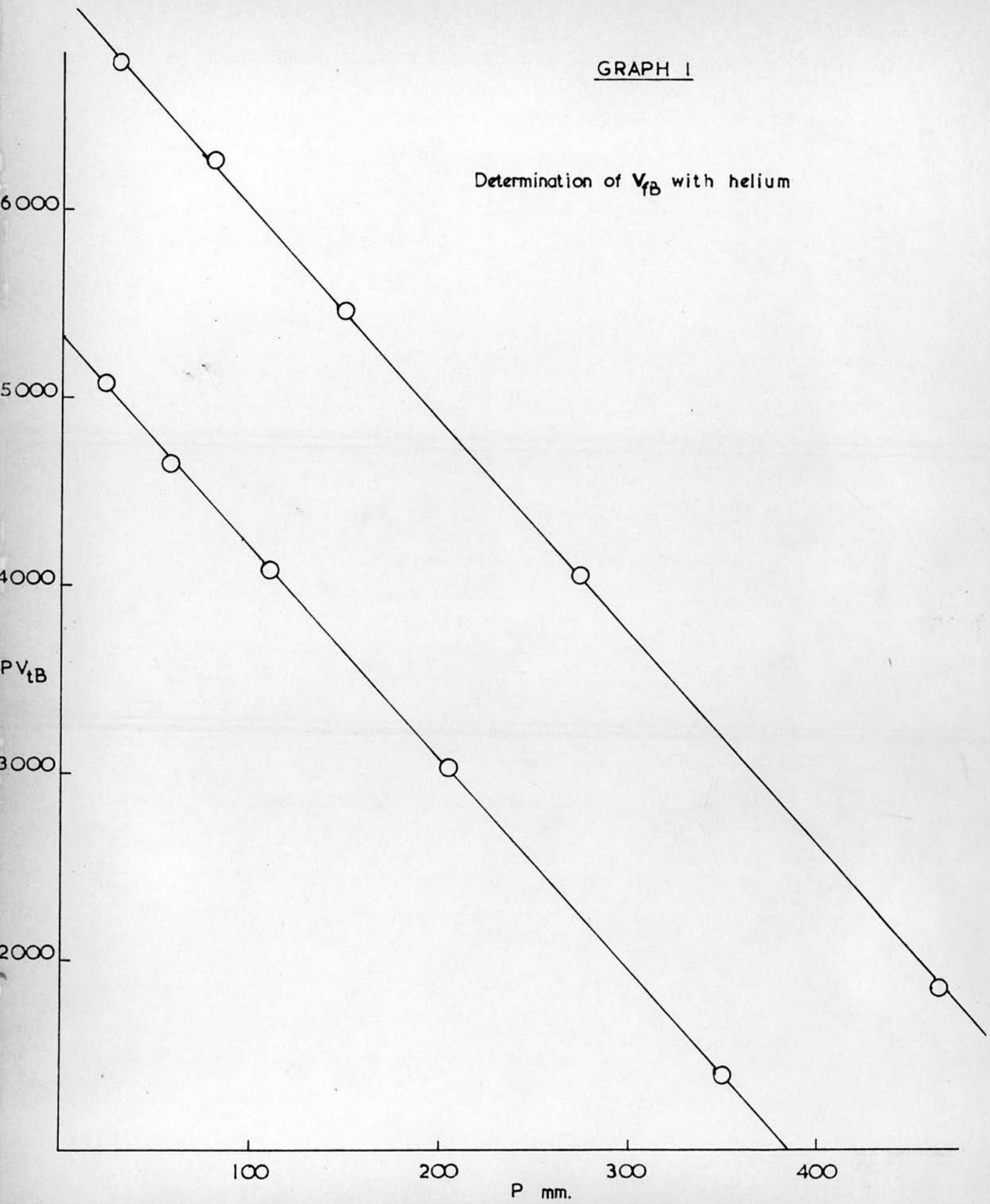
GRAPH 1
Determination of V_{fB} with helium
6000
5000
4000
3000
2000
PV_{tB}
100
200
300
400
P mm.

Determination of the Free Volume of the Adsorption System with Helium.

Temperature of the gas burette = 20.5 °C

	1st determination		2nd determination	
V_{tB} ml	P mm	PV_{tB}	P mm	PV_{tB}
-	468.6		628.4	
3.95	350.5	1384	469.8	1856
14.79	204.8	3029	273.8	4049
36.46	111.7	4072	149.5	5451
79.93	58.1	4644	77.9	6227
217.86	23.2	5055	31.0	6754

From Graph 1 ,

1. Slope = $- V_{fB}$ = - 11.10

2. Slope = $- V_{fB}$ = - 11.20

By average of points ,

1. Slope = $\frac{\bar{y}_2 - \bar{y}_1}{\bar{x}_2 - \bar{x}_1}$ = - 11.05

2. Slope = - 11.12

∴ Volume Free Space = 11.12 ml .

Burette reference mark	Vol. of System ml.	Volume factors
0	11.12	f_{V_0} = 4.00
1	15.07	f_{V_1} = 5.41
2	25.86	f_{V_2} = 9.28
3	47.58	f_{V_3} = 17.09
4	91.05	f_{V_4} = 32.72
5	228.98	f_{V_5} = 82.30

GRAPH 2

Catalyst XIV 3.9 g

Argon adsorption at 77.9°A

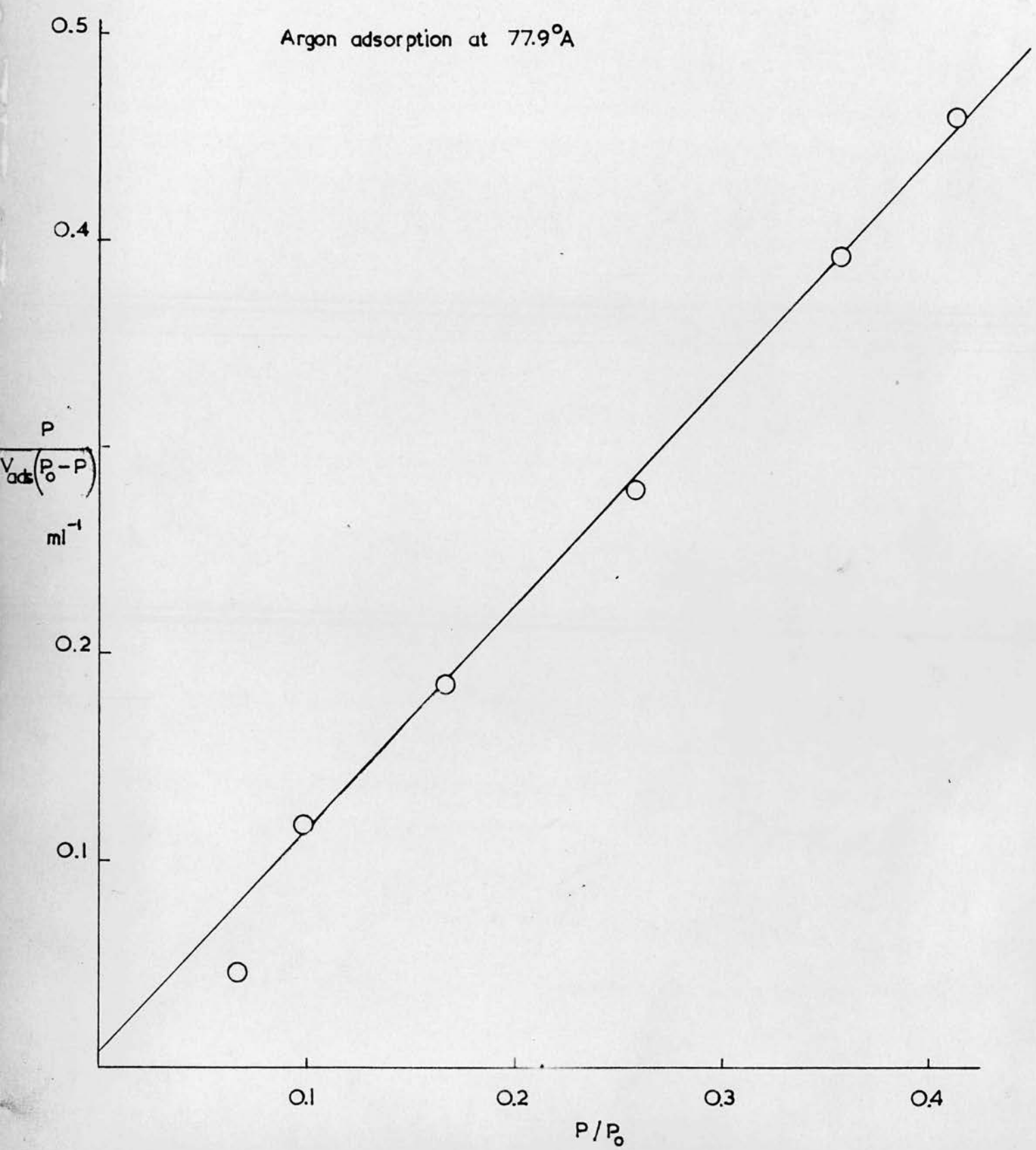

Example of a Surface Area Determination

Specimen - Catalyst XIV 3.9 g

Calibration of Adsorption Bulb Free Volume with Helium

Temperature of gas burette = 21.0 °C , Temperature of liquid nitrogen = 77.9 °A .

Stopcock A closed, on zero in gas burette, P(He) = 685.5 mm. V_T = 8.183 ml.

Stopcock A opened, on zero in gas burette, P(He) = 356.0 mm. V_R = 4.250 ml.

Volume of helium at N.T.P. in adsorption bulb, f_A(He)= 3.933 ml.

Volume factor for the adsorption, f_A , = $\frac{V_A}{P_1}$ = 0.001103

Adsorption of Argon

Temperature of gas burette = 20.5 °C , Temperature of liquid nitrogen = 77.9 °A .

Vapour pressure of argon at 77.9 °A , P_o , = 240 mm.

Stopcock A closed, on No 5 in gas burette, P(A) = 13.66 mm. V_T = 3.806 ml.

Stopcock A opened,

Burette Reference No.	Press. of Argon mm.	Vol. in G.B. V_R ml.	Vol. in bulb V_A ml.	Vol. ads. V_{ads} ml.	$\frac{P}{V_{ads}(P_o - P)}$	$\frac{P}{P_o}$
5	10.72	2.986	0.118	0.702	0.067	0.045
4	23.80	2.613	0.263	0.930	0.118	0.099
3	40.16	2.272	0.444	1.090	0.185	0.167
2	62.22	1.870	0.688	1.248	0.280	0.259
1	85.80	1.441	0.948	1.417	0.393	0.357
0	99.00	1.184	1.094	1.528	0.460	0.413

From the plot of $\frac{P}{V_{ads}(P_o - P)}$ against $\frac{P}{P_o}$, (Graph 2)

Intercept = 0.01 Slope = 1.08

Volume of argon required for a monolayer = $\frac{1}{S + I}$ = 0.92 ml.

∴ Area of specimen = 3.88 × 0.92 = 3.56 m^2.

∴ Surface Area of Catalyst XIV = 3.56 / 3.90 = 0.91 m^2/g.

Table 2

Catalyst	Atom percent Copper	Surface Area m^2 / g
I	0	1.10
II	13.0	0.54
III	20.1	0.70
IV	29.3	0.60
VI	49.6	0.60
IX	63.8	0.58
XII	69.2	0.40
XIII	82.2	0.66
XIV	92.6	1.00
XV	100	0.25
XVA	100	0.22

X - ray Diffraction

X-ray powder diffractograms of three alloys and the pure metals were taken for comparison with the results of Hall and Alexander [30], and others[7,8,10,12] and to check that the alloys were in fact true solid solutions.

A Phillips x-ray diffractometer was used with copper K_{α} radiation at 30 KV. and 12 mA . The Gieger counter voltage was 1650 V., and the specimen scanned from 10 to 160 °. This method enabled measurement of the diffraction angle to be made to an accuracy of + or - 0.1° and the lattice spacing to + or - 0.002 Angstrom.

The work Owen and Pickup [7] on fused alloys of copper and nickel was substantiated by that of Hall and Alexander [30] who used alloys prepared from the basic carbonates of copper and nickel. Their results show a gradual variation of lattice spacing with composition until about 66 atom percent copper is reached, whereafter a slight change in slope on the lattice spacing - - composition curve is noted. Coles [35,36] however claims that no discontinuity in slope appears at this point, but that there is an appreciable change of slope at 33 atom percent copper, this being the composition where the Curie point is, at or near room temperature. From this observation, Coles suggests that the variation in slope is connected with the Curie point and not with the filling of the d-band.

As far as can be ascertained from the results given below the alloys used in the present work are homogeneous solid solutions. The results show the same deviation from Vegard's law which both Owen and Pickup, and Hall and Alexander found at about 60 atom percent copper. The results given have been measured in Angstrom units, and the results of Owen and Pickup quoted, have been corrected from kX units to Angstroms. Since the lattice spacing of alloys between 30 - 40 percent copper was not investigated nothing can be said about the deviation noticed by Coles.

GRAPH 3

Lattice Spacing / Composition

Straight lines represent the work of Owen and Pickup

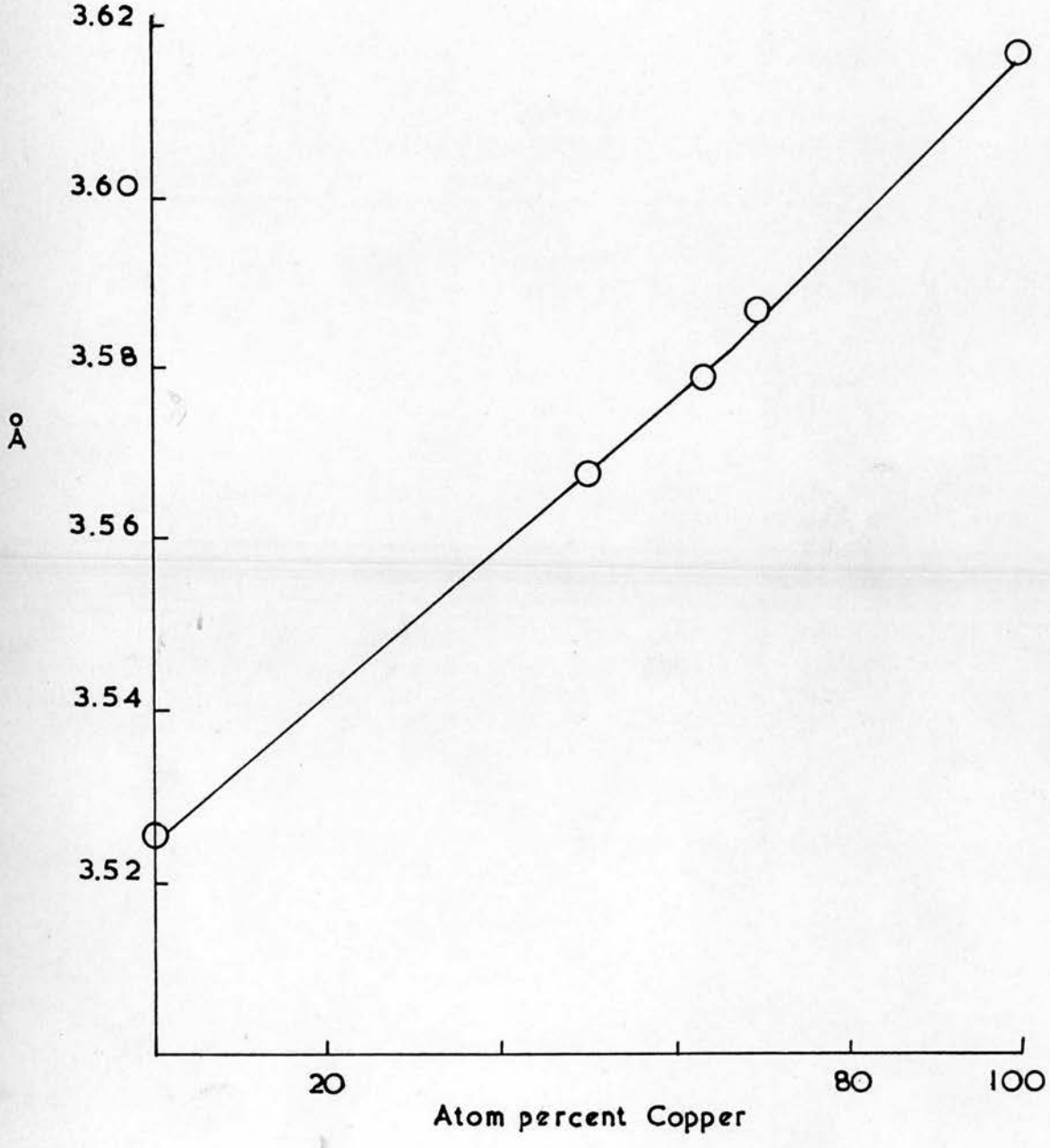

TABLE 3 X-ray Diffraction Results

Copper target 30 KV. 12 mA. Unfiltered

K_{α_1} radiation λ = 1.54051 Å.

K_{α_2} radiation λ = 1.54433 Å.

Catalyst	Atom percent Copper	2 θ	K_α	d_{331}	d_{420}	a Å.	a (Owen and Pickup corrected to Å)
XV	100	136.20	1	0.8302		3.619	3.616
		136.90	2	0.8297		3.617	
		144.40	1		0.8090	3.618	
		145.25	2		0.8086	3.617	
XII	69.2	138.80	1	0.8229		3.587	3.585
		139.60	2	0.8223		3.584	
		147.50	1		0.8023	3.588	
		148.50	2		0.8019	3.586	
IX	63.8	139.45	1	0.8211		3.579	3.579
		140.25	2	0.8205		3.577	
		148.60	1		0.8001	3.578	
		149.70	2		0.7995	3.576	
VI	49.6	140.40	1	0.8186		3.568	3.567
		141.10	2	0.8184		3.567	
		149.80	1		0.7978	3.568	
		150.80	2		0.7974	3.566	
I	0	144.40	1	0.8091		3.527	3.524
		145.30	2	0.8095		3.524	
		155.40	1		0.7884	3.526	
		156.85	2		0.7877	3.523	

Magnetic Susceptibility Measurements

Measurements of the magnetic susceptibility of alloys are useful in giving an indication of the presence of unpaired electrons due to holes in the d-band. For this reason, measurements of the susceptibilities of pure copper and of four alloys up to 50 atom percent nickel were made by the Gouy method. Weighings were made on a Stanton model SM12 balance. The electromagnet and stabilised power pack were supplied by Newport Instruments. A constant field strength of about 8000 oersted was used and the Gouy tube calibrated with $Hg(Co(CNS)_4)$ [37]. All measurements were carried out at room temperature. A slight dependence of the susceptibility on field strength was noted during the measurements on all the catalysts. This, according to Pugh and Ryan [38] is due to ferromagnetic impurities. Pugh, Ryan and Smoluchowski [39] have also shown that the susceptibilities of alloys of less than 27 atom percent nickel are temperature independent. Any comparison of kinetic results with susceptibility in this region of alloy composition therefore needs no temperature correction.

The results obtained are in agreement with those of Kaufmann and Starr [40] and also those of Best and Russell [11] for similarly prepared alloys. All these results show that the decrease in susceptibility at 60 atom percent copper as predicted by the band theory of Mott and Jones [6] is more gradual than the theory predicts. These results do not compare with those obtained by Reynolds [41] who, for skeletal copper-nickel alloys and to a lesser degree for those prepared by oxide reduction, found that the magnetic susceptibility fell to an insignificant value for all alloys of copper content greater than 40 atom percent copper. The susceptibilities of the foils used by Dowden and Reynolds [9] fall more into line with the results of Kaufmann and Starr, and Best and Russell.

Measurements with the Gouy Balance

The 3 mm. diameter Pyrex Gouy tube, having a reference mark 9 cm. from the closed end, was suspended by aluminium wire so that the bottom was on the axis of the horizontal pole-pieces of the magnet. Before any weighings were carried out (with the tube empty or filled, or with the magnet switch on or off), the tube was left suspended for ten minutes, to allow it to reach the temperature of the surrounding air and as necessary to allow the magnetic field to become uniform.

The tube was weighed empty with the magnet switched off and then again with it on. In this way the diamagnetic correction for the tube was obtained. The volume of the tube was then calibrated by filling it to the reference mark with water and weighing with the magnet off. The tube calibration constant was found by use of $Hg(Co(CNS)_4)$, the magnetic susceptibility of which is accurately known.

The specific susceptibility of the sample is given by [42],

$$10^6 \chi = \frac{\alpha + \beta F'}{W}$$

where $F' = F - \delta$

α = constant for displaced air = 0.029 × specimen volume

β = tube calibration constant

W = weight of specimen

F' = force on specimen

F = observed force

δ = diamagnetic correction for the tube

By convention α, F and δ are measured in mg. and W in g.

FIGURE 3

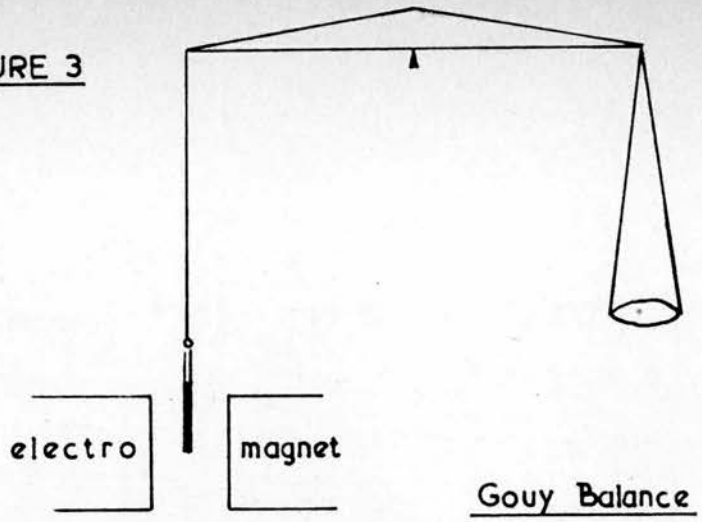

Gouy Balance

GRAPH 4

Magnetic Susceptibility / Composition

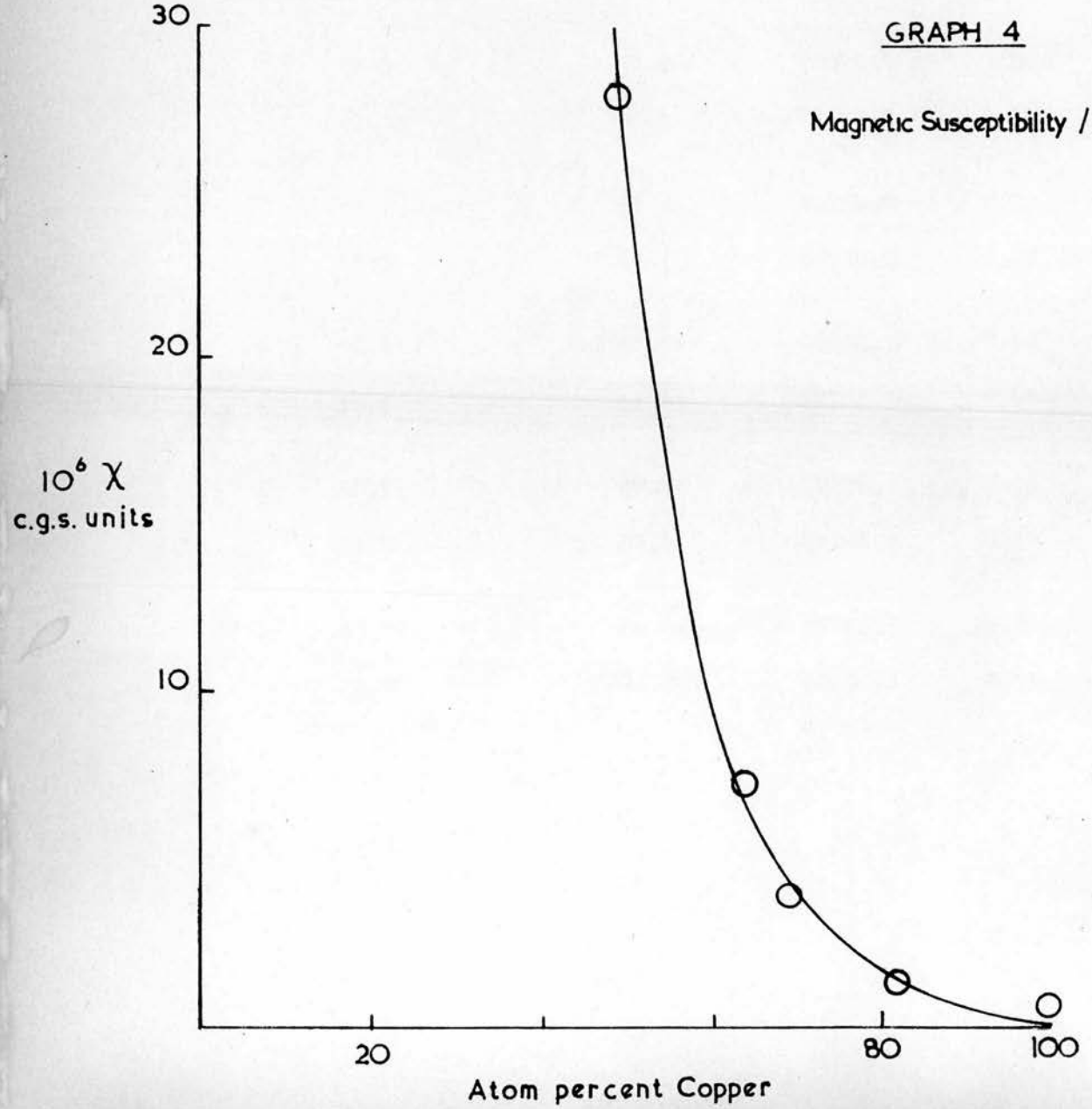

TABLE 4

Specific susceptibility of $Hg(Co(CNS)_4)$ = 16.44×10^{-6} cgs units. [37]

Specimen volume = 0.68117 ml.

α = 0.02 mg.

δ = -2.68 mg.

β = 0.314

Catalyst	Atom percent Copper	Wt. used g.	Force observed mg.	Specific susceptibility $10^6\chi$ cgs units.
XV	100	0.97197	-0.53	0.715
XV	100	0.98897	-0.50	0.712
XIII	82.2	0.93260	1.17	1.32
XIII	82.2	0.95083	1.35	1.36
XII	69.2	1.58144	16.35	3.80
XII	69.2	1.55737	16.13	3.80
IX	63.8	1.80177	38.83	7.33
IX	63.8	1.83349	40.05	7.41
VI	49.6	1.13237	96.93	27.64
VI	49.6	1.15864	100.40	27.80

FIGURE 4

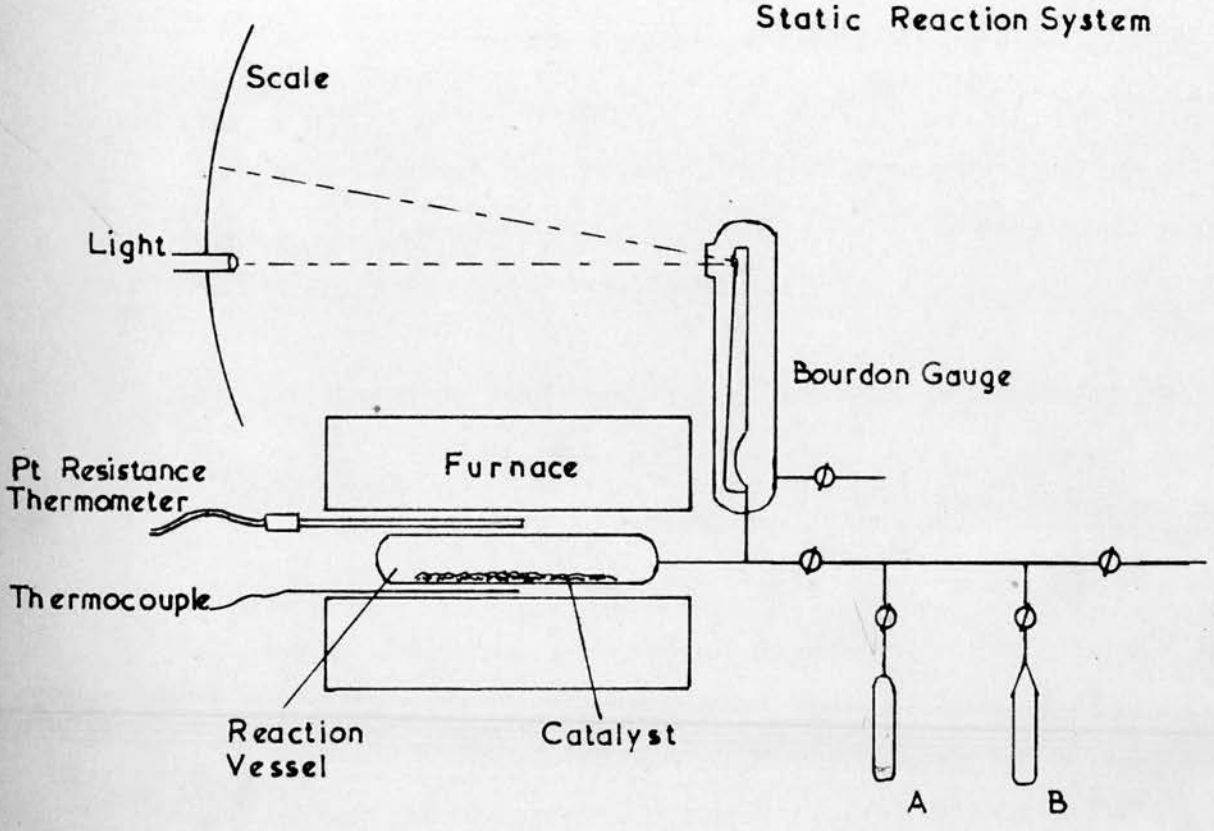
Static Reaction System
Scale
Light
Bourdon Gauge
Furnace
Pt Resistance Thermometer
Thermocouple
Reaction Vessel
Catalyst
A
B

Reaction System for Kinetic Measurements

Figure 4 shows the static system used for the kinetic experiments. The whole system was constructed of 'Pyrex' glass, 'Apiezon' L and M greases being used to lubricate all joints and stopcocks respectively.

Pumping System

The pumping system consisted of a three stage mercury diffusion pump backed by a 'Speedivac' rotary oil pump and gave pressures less than 10^{-5} mm. Hg. Two liquid nitrogen traps were used in the system to minimise any poisoning of the catalysts by hydrocarbon and mercury vapours from the pumping system.

Reaction Vessel

The reaction vessel was a horizontal cylindrical tube, 28 mm. in diameter and 80 ml. volume. Initially this was open at one end so that hydrogen could be flowed over the catalyst during its preparation. The other end was sealed to 2 mm. internal diameter capillary tubing connected directly to a Bourdon gauge. A new but similar reaction vessel was used for each catalyst.

Bourdon Gauge

This was fitted with an optical lever system. In this way the pointer deflection was magnified and could be read on a metre scale, a pressure change of 1 mm. Hg giving a deflection of approximately 7 mm. on the scale. This deflection was linear with respect to pressure over the range of pressures used in the kinetic measurements. The gauge was calibrated against a simple mercury manometer.

Furnace

The furnace consisted of a silica tube 45 cm. long and 4 cm. internal diameter, which was heated electrically by means of three windings of 26 gauge /

/ nichrome wire (resistance 2.37 ohms per foot) connected in series. The whole was suitably insulated and enclosed in asbestos board. The furnace was mounted on horizontal rails so that it could be moved easily to allow replacement of the reaction vessel. The temperature of the furnace was controlled to within 0.1 °C by means of an electronic controller and a Sangamo Weston Platinum Resistance Thermometer Model S110 placed in contact with the reaction vessel.

Temperature Measurement

The temperature of the reaction vessel was measured by means of a thermocouple, the junction of which was kept in contact with the wall of the reaction vessel. The cold junction was placed in ice in a 'Thermos' flask. The thermocouple was constructed from British Driver Harris T_1 / T_2 thermocouple alloys the junctions being electrically welded under an atmosphere of nitrogen. The voltage from the thermocouple could be read to 0.001 mV on a Type P3 potentiometer manufactured by the Croyden Precision Instrument Company.

The thermocouple was calibrated in steps of 20 °C from 20 °C to 500 °C against a standard Pt / Pt Rh thermocouple.

Formic Acid Decomposition

Purification and Storage of Formic Acid

'Analar' formic acid was further purified by completely freezing the sample with salt and ice and then allowing it to thaw. When half the sample had melted, the liquid was poured off and the remaining solid allowed to melt. This was repeated five times until a constant melting point of 8.2 °C was obtained. This value for the melting point agrees well with that given by Coolidge [43] but is 0.2 °C lower than that given by Ewins [44].

By use of traps A and B (Figure 4), the purified formic acid was distilled three times under vacuum at room temperature, the distillate being condensed each time in a trap at -78 °C. During each distillation the first and the last twenty percent of the liquid were rejected by pumping. The formic acid thus obtained was stored at -78 °C using a 'Cardice' - acetone bath. Before using the formic acid in any run, it was degassed for one minute by pumping while it was melting.

Procedure for each run

The reaction vessel containing the catalyst was evacuated continuously between each run, the time varying from thirty minutes to sixty hours. In this time a pressure of at most 10^{-5} mm. Hg was attained. If at any time the pressure was greater than this, a slight falling off in the activity of the catalyst was noticed.

After evacuation was completed, the single tap to the static system (reaction vessel and Bourdon Gauge) was closed. The still solid formic acid was then pumped for one minute and the tap at the end of the manifold to the pumping system closed. The formic acid was allowed to come up to room temperature and in this way the manifold filled with formic acid vapour.

By opening the tap to the static system a pressure of up to 30 mm Hg of /

/ formic acid vapour could be introduced, after which the tap was closed. The pressure shown on the Bourdon gauge on closing the tap was taken as the initial pressure. Pressure readings were taken every two minutes and the reaction followed in most cases to 50 percent and in some cases to 100 percent decomposition.

Kinetics of the Decomposition

The decomposition of formic acid was carried out on seven alloys of copper and nickel and on the pure metals at temperatures ranging between 80 and 200 °C. The reaction was also carried out at three different initial pressures of formic acid for each temperature studied, these being approximately 25 , 17 , and 10 mm Hg.

Blank runs in the absence of catalyst showed that the 'Pyrex' reaction vessel did not catalyse the decomposition below 270 °C, and Blake and Hinshelwood [45] have shown that homogeneous decomposition of formic acid does not take place under these experimental conditions below 400 °C. The results reported therefore clearly relate only to the metal-catalysed reaction.

The decomposition proceeded initially as a zero order reaction on all the catalysts used, but in the later stages of the reaction (approximately after 40 percent decomposition) appreciable inhibition was found. This was shown by a gradual fall off in rate until the limiting value of pressure increase was reached, the high nickel alloys showed more inhibition by the products than the copper rich alloys.

The reaction rate for any one temperature was determined by at least three decompositions at different initial pressures. The rate of reaction was found to be directly proportional to the weight of catalyst used for the /

/ decomposition and so to the surface area of the catalyst. By removing nine-tenths of the catalyst it was possible to follow the reaction at higher temperatures and so extend the range of temperature at which the reaction could be studied.

Correction for the dimerisation of formic acid was made for all reactions carried out at 110 °C or below from the data given by Coolidge [46], and Ramsperger and Porter [47].

For the reversible reaction

$$(HCOOH)_2 \rightleftharpoons 2\,HCOOH$$

the equilibrium constant is given by

$$K = \frac{4\alpha^2}{1-\alpha^2} \cdot P$$

where α = degree of dissociation and P = total pressure of monomer and dimer. At temperature T, the equilibrium constant is given by Coolidge [46]

$\log K = 10.755 - 3090 / T$, and thus the value of α at any time t after the start of the reaction at temperature T can be calculated from,

$$\alpha_t = \sqrt{\frac{K}{K + 4(P_{M_t} + P_{D_t})}} \qquad (A)$$

where P_{M_t} and P_{D_t} are respectively the monomer and dimer partial pressures at time t.

The overall reaction is assumed to be,

$$(HCOOH)_2 \rightleftharpoons 2\,HCOOH \longrightarrow 2\,H_2 + 2\,CO_2$$

and thus $P_o = P_{M_o} + P_{D_o}$

$$P_t = P_{M_t} + P_{D_t} + 2\,P_{H_2 t}$$

when the subscript zero refers to zero time and subscript t to time t , P is the measured total pressure and P_{H_2} is the hydrogen pressure.

We also have the measured increase in pressure ΔP

$$\Delta P = P_{H_2} + P_{D_o} - P_{D_t} = P_t - P_o$$

whence

$$P_{H_2} = P_{M_o} - P_{M_t} + 2P_{D_o} - 2P_{D_t} .$$

Since $\Delta P = P_{H_2} + P_{D_o} - P_{D_t} = P_{H_2} + \frac{1 - \alpha_o}{1 + \alpha_o} \cdot P_o - \frac{1 - \alpha_t}{1 + \alpha_t} \cdot (P_{M_t} + P_{D_t})$,

it can be shown that

$$\alpha_t = \frac{2(P_{M_t} + P_{D_t}) - \frac{2P_o}{1 + \alpha_o} + P_{H_2}}{\frac{2P_o}{1 + \alpha_o} - P_{H_2}} \qquad (B)$$

The above two equations for α_t may now be combined to give a single equation, which may be solved to give P_{H_2} for any desired value of $(P_{M_t} + P_{D_t})$. The solution is, however, cumbersome and so the following procedure was therefore adopted.

For the known initial pressure P_o of formic acid at time zero, the value of α_o was calculated from equation (A). Then from equation (B), the value of P_{H_2} was calculated for chosen values of $(P_{M_t} + P_{D_t})$, the appropriate value of α_t having been obtained from equation (A). Corresponding values of $P_t = P_{M_t} + P_{D_t} + 2P_{H_2}$ were thus obtained.

The experimental P_t - time graph can therefore be converted into a P_{H_2} - time graph from which the true zero order rate constant is obtained. Since the P_t - time graph was linear for about one third of the decomposition, it was sufficient to calculate only a single value of P_{H_2} for $(P_{M_t} + P_{D_t}) = \frac{2}{3} P_o$, and join the corresponding point to the origin with a straight line.

The detailed procedure was as follows.

At 90 °C, K = 176 , giving α_o = 0.785 when P_o = 27 mm. from equation (A). For $(P_{M_t} + P_{D_t})$ = 17 mm., α_t = 0.85 , and thus from equation (B), P_{H_2} = 11.9 mm. P_t is therefore 17 + 2 × 11.9 = 40.8 mm. From the experimental P_t - time graph,, the value of t when P_t = 40.8 mm.is obtained, and thus the true zero order rate constant is 11.9 / t , the units being mm. formic acid per unit time.

If the dimer - monomer correction is omitted, then from the experimental P_t - time graph, the apparent zero rate constant would be ,

$$\frac{\Delta P}{t} = \frac{40.8 - 27}{t} = \frac{13.8}{t}$$

and thus the correction amounts to a reduction of the apparent constant by about 14 percent.

Above 110 °C, α is greater than 0.95 and so very little dimer exists and the correction becomes insignificant.

Attempts were made to obtain a reaction rate constant for the complete decomposition from equations derived from the Langmuir adsorption isotherm. This approach is similar to that used by Walton and Verhoek [48] who obtained reaction rate constants in this way for the decomposition of formic acid at pressures between 10 and 50 mm. Hg on evaporated nickel films.

The results obtained for the alloys however did not fit their equation nor did they fit any equation derived in a similar way. Arrhenius plots were therefore obtained from the zero order rates.

Analysis of the Products of the Decomposition

The decomposition products from several runs were allowed to expand through a trap at -78 °C into an infra - red gas absorption tube.

With a Hilger H 800 spectrophotometer, only carbon dioxide was detected.

By means of a pallado - sulphite detector tube [49], very small amounts of carbon monoxide were observed.

This suggests that the decomposition proceeds mainly as a dehydrogenation, but other experiments [50] using a flow system showed by gas chromatographic analysis that initially about twenty percent carbon monoxide was present.

These results however, are not conflicting since any carbon monoxide formed initially could be catalytically converted to carbon dioxide by the water gas shift reaction, the equilibrium lying far to the carbon dioxide side at the temperatures concerned [20].

$$HCOOH \longrightarrow H_2O + CO$$

$$H_2O + CO \rightleftharpoons H_2 + CO_2$$

Thus at the end of the reaction in a static system, very little carbon monoxide appears in the products.

Results of the Formic Acid Decomposition

TABLE 5

In this table a selection of the kinetic measurements of the formic acid decomposition on copper, nickel and an alloy of 49.6 atom percent copper is given.

They show the conversion as a function of time at a fixed temperature for various initial vapour pressures of formic acid.

The corresponding graphs, (Graphs 5, 6, and 7) show the wide region in which the curves coincide before the limiting pressure values are reached. From the curves it can be seen that the reaction is initially of zero order. This pattern persisted throughout the range of alloys used.

TABLE 5

Catalyst	I			VI			XV		
Composition	0 % Cu			49.6 % Cu			100 % Cu		
Weight	3.30 g			3.25 g			3.75 g		
Surface Area	3.6 m^2			2.0 m^2			1.0 m^2		
Bourdon Gauge Factor	5.10			5.35			5.35		
Temperature °C	110 °			120 °			170 °		
Initial Pressure P_o (scale divisions)	128	102	90	132	95	53	133	92	53
Time minutes	Pressure Increase ΔP in scale divisions								
1	6	5.5	5.5	7	7	7	3	3	3
2	12	11	10.5	15.5	15	15	6	6	6
3	16	15	14.5	24.5	24	23			
4	20	19	18.5	32.5	32	30	12	12	11.5
5	24	23	22.5	39.5	39.5	36			
6	28	27	26.5	48	47	41	18	18	17
8	32	30.5	29.5	62	61	48	23.5	23.5	22.5
10	36	34	32.5	76	73	52	29	29	27
12	40	37.5	35.5	88	83		34	34	31.5
14	44	41	38	99	89		40	39	35.5
16	48	44	40.5	109			45	44	38.5
18	51.5	47	42.5				50.5	49	41.5
20	54.5	50					55.5	53	
25							68.5	63	
30							80.5		

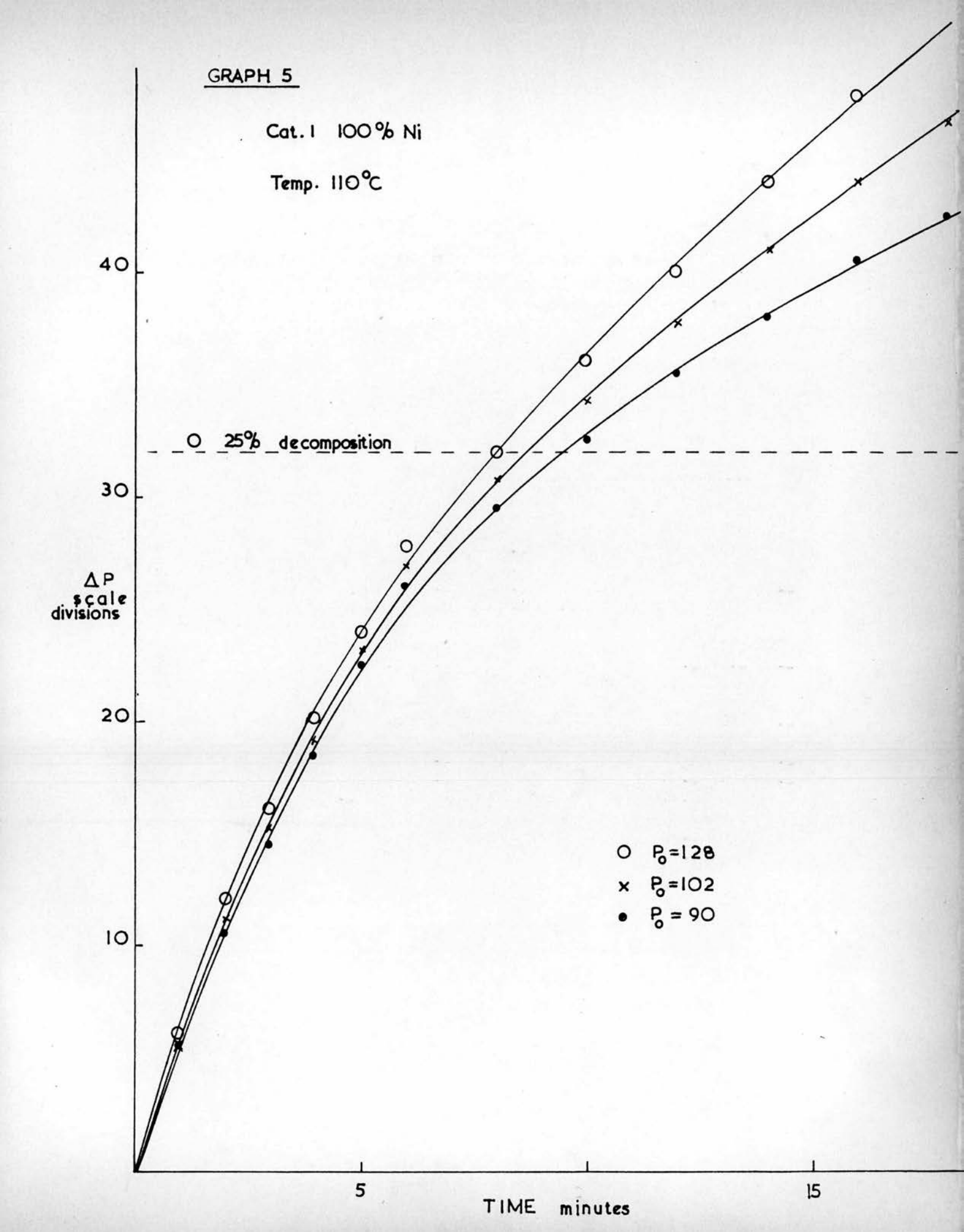
GRAPH 5
Cat. 1 100% Ni
Temp. 110°C
40
30
20
10
ΔP scale divisions
25% decomposition
P_o=128
P_o=102
P_o = 90
5
15
TIME minutes

GRAPH 6

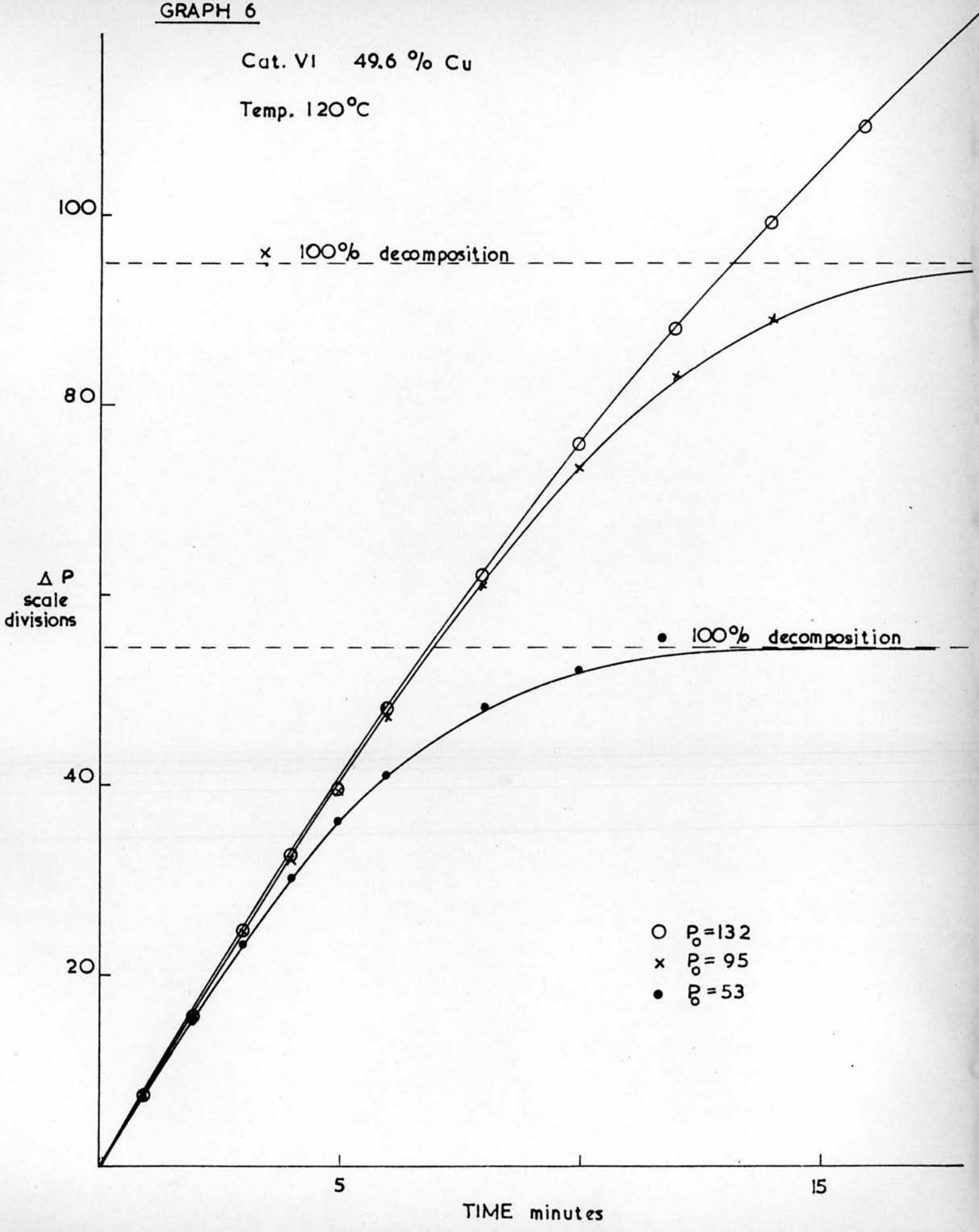
Cat. VI 49.6 % Cu
Temp. 120°C
100
× 100% decomposition
80
Δ P
scale
divisions
40
• 100% decomposition
20
O P_o=132
× P_o= 95
• P_o=53
5
15
TIME minutes

GRAPH 7

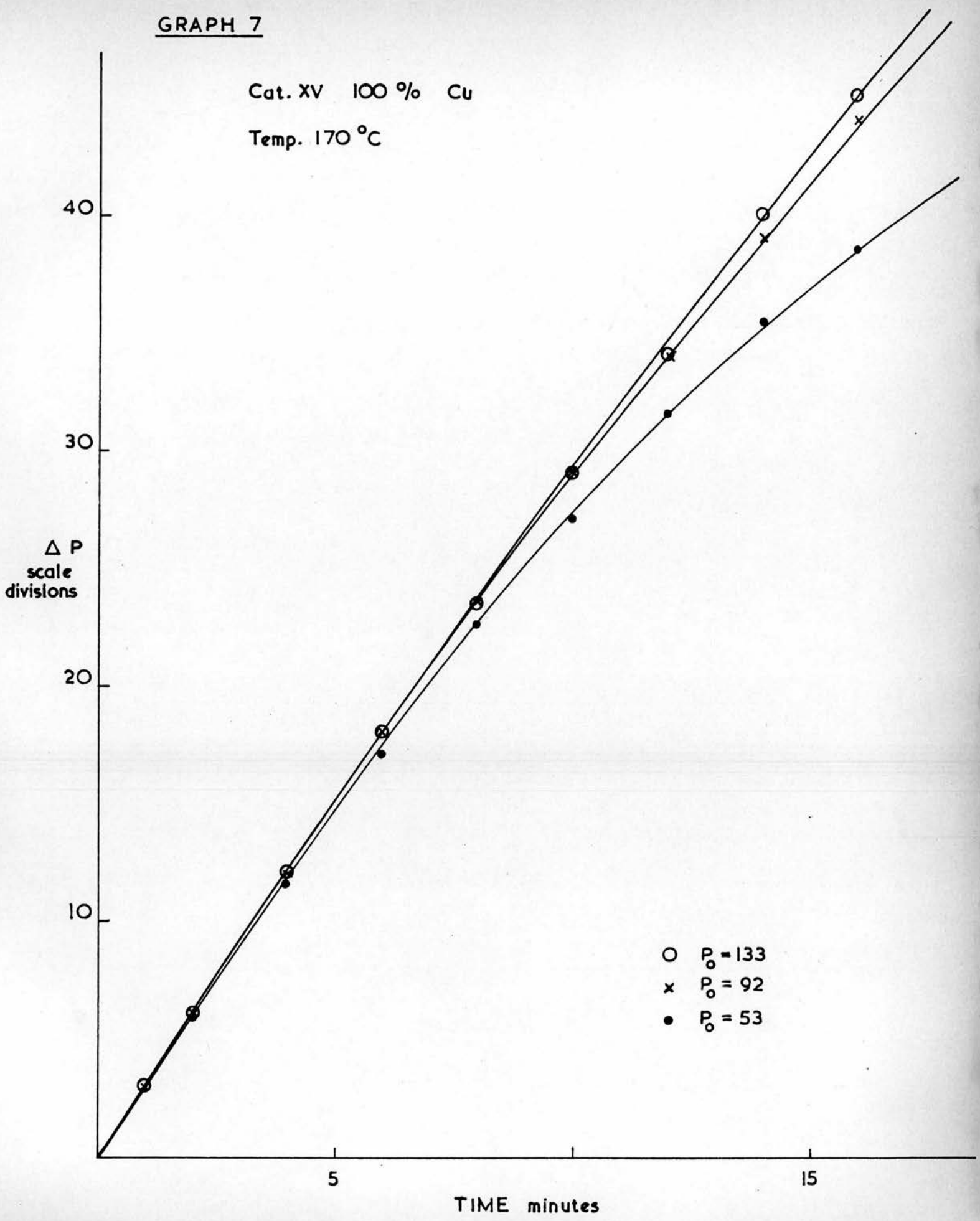
Cat. XV 100 % Cu
Temp. 170 °C
40
30
20
10
Δ P
scale
divisions
5
15
TIME minutes
○ P_o = 133
× P_o = 92
● P_o = 53

TABLE 6

The reaction rate constants for the decomposition on all the catalysts used are given in this table together with the respective temperatures.

The rates have been calculated in molecules site^{-1} sec.$^{-1}$ assuming that each metre^2 of surface contains 1.6×10^{19} sites. This figure is obtained assuming every surface atom to be a site and nickel to have a face-centred cubic structure of side 3.51 Å. Thus there is one atom every 2.47 Å, so one atom is associated with an area of 6.1 Å^2.

The pre-exponential factors obtained from Arrhenius equations for the various catalysts have the same units, molecules site^{-1} sec.$^{-1}$.

The activation energies obtained from linear Arrhenius plots, illustrated in Graph 8, have been calculated by the method of least squares.

The variation of activation energy and activity as a function of composition have been shown graphically in Graphs 9 and 10. In the log Rate - composition graph the rates have been interpolated, and in some cases extrapolated, from Arrhenius plots.

A plot has also been made, Graph 11, of activation energy against the logarithm of the pre-exponential factor to show any compensation effect which might be present.

TABLE 6

10^4 × (Reaction Rate in molecules site^{-1} sec.$^{-1}$)

Temperature °C	I	III	IV	VI	IX	XII	XIII	XIV	XV	XVA
80					0.4					
90	1.2				1.2	2.7				
100	2.6	2.1		2.3	3.4	5.8	1.5			
110	6.2	5.7	2.3	6.5	8.3	13	3.3			2.2
120	14	12	7.5	15	17	33	6.6	1.0		5.8
130	27	32	16	31	36	82	14	2.1		10
140	64	49	30	58		170	30	4.5		21
150	130	100	53	140		300	54	8.5	3.4	54
160	400	190	72	220			130	17	5.0	100
170		330	140	360			300	32	9.4	180
180			270				580	74	13	
190			500					91	23	
200								130	39	
Activation Energy kcal.mole^{-1}	24.2 ±0.6	23.9 ±0.5	20.8 ±0.8	23.8 ±0.6	26.6 ±1.5	26.1 ±0.6	23.4 ±0.4	24.7 ±0.6	20.3 ±0.9	25.3 ±0.6
log A	10.62	10.37	8.45	10.36	11.95	12.04	9.87	9.69	6.95	10.78

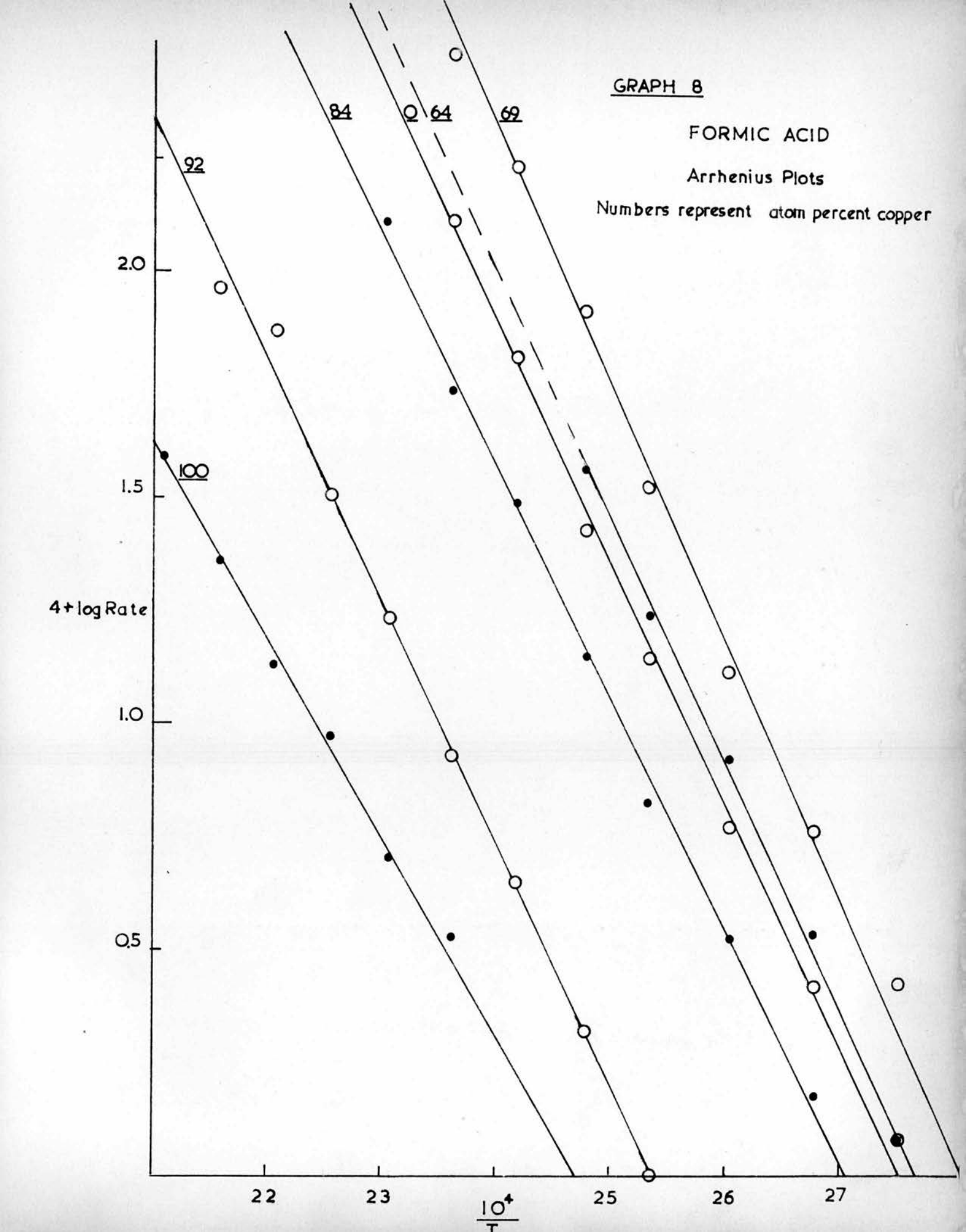
GRAPH 8
FORMIC ACID
Arrhenius Plots
Numbers represent atom percent copper
92
84
64
69
100
2.0
1.5
1.0
0.5
4+log Rate
22
23
25
26
27
$\frac{10^4}{T}$

GRAPH 9

FORMIC ACID

Activation Energy / Composition

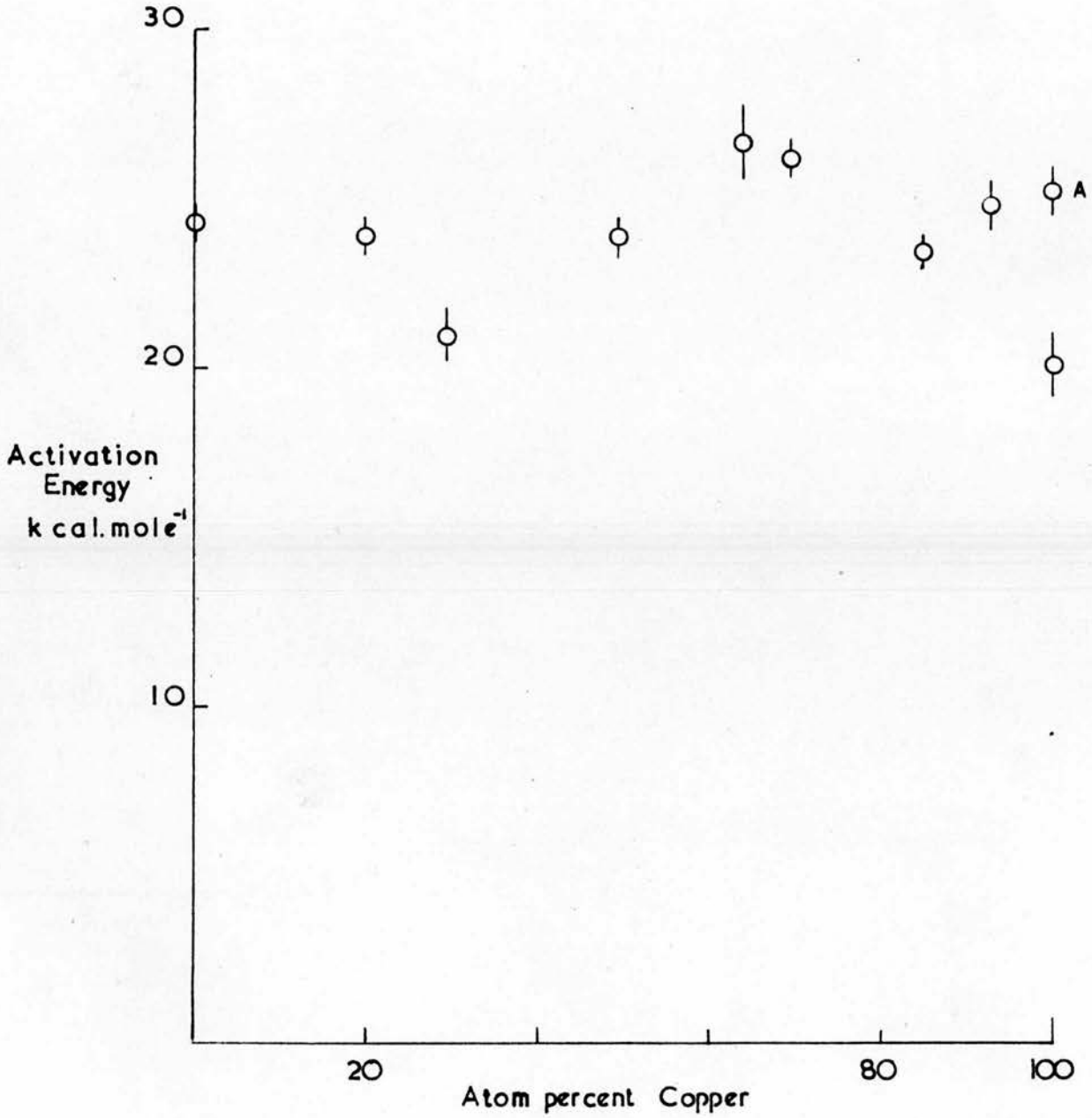

GRAPH 10

FORMIC ACID

Activity Pattern

Rate measured in molecules site^{-1} sec.$^{-1}$

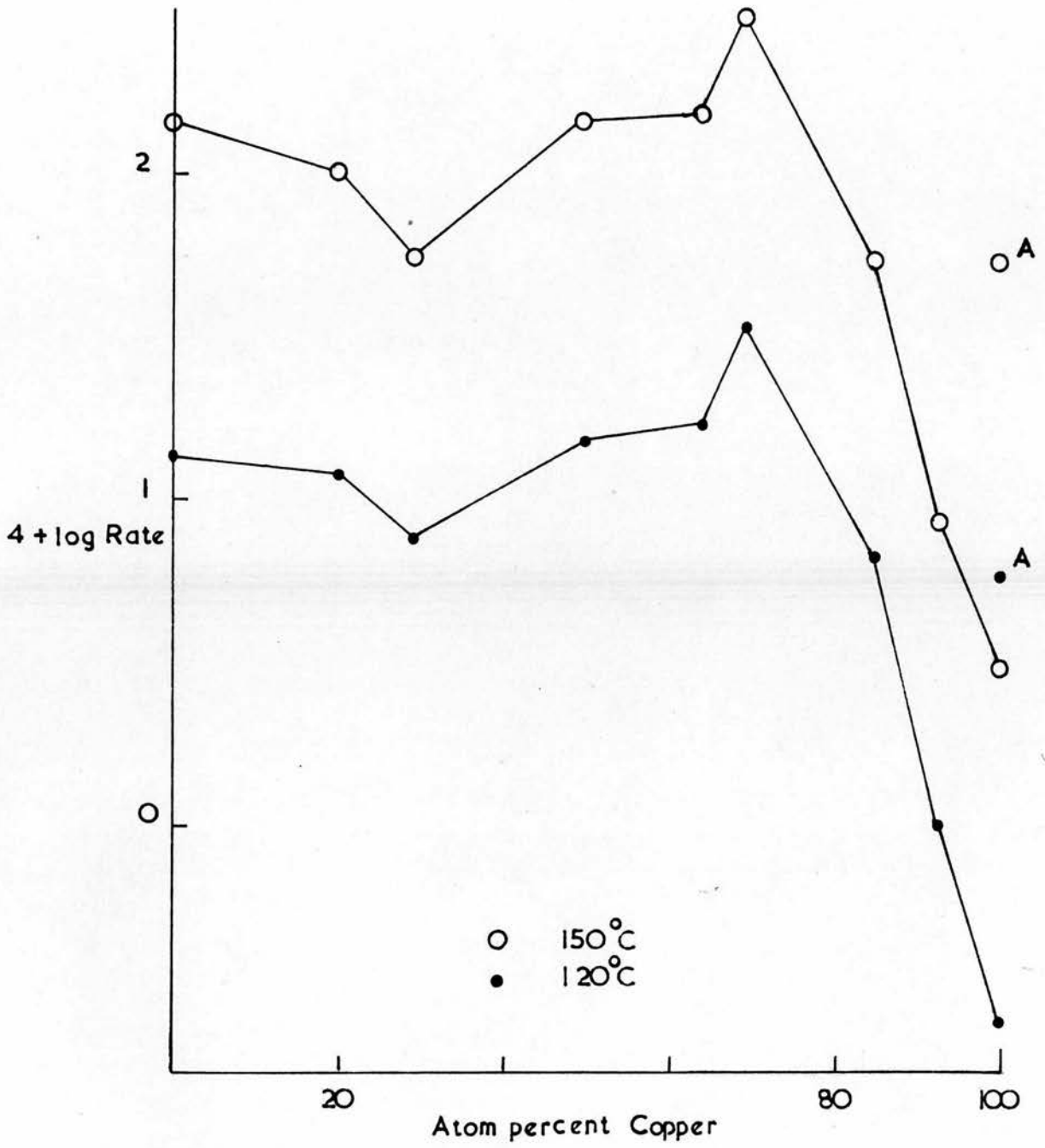

GRAPH II

FORMIC ACID

Compensation Effect

Numbers represent atom percent copper

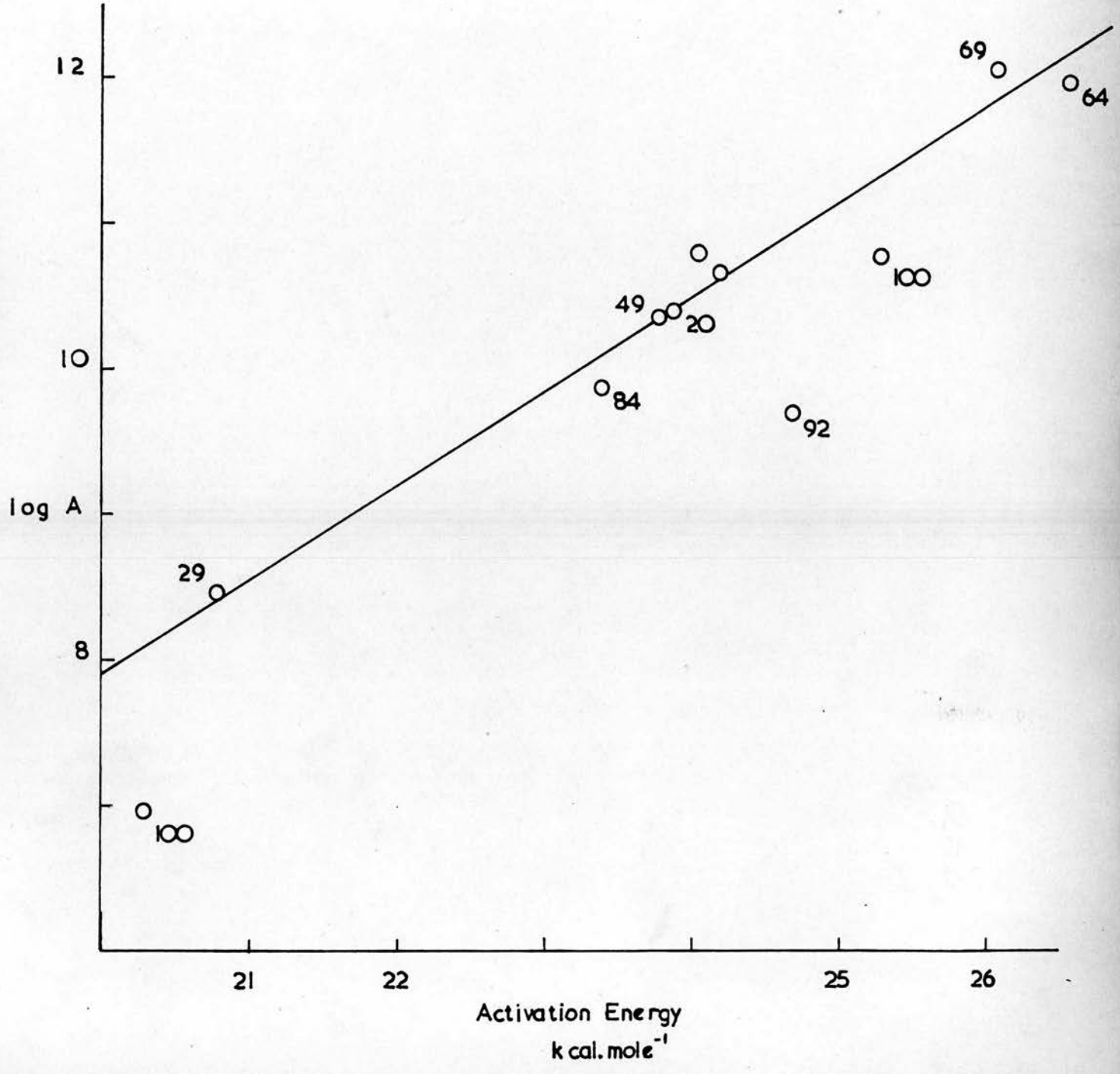

Methanol Decomposition

Purification and Storage of Methanol

'Absolute' methanol was dried in the following way.

$$Mg + 2\,CH_3OH \longrightarrow H_2 + Mg(OCH_3)_2$$

$$Mg(OCH_3)_2 + 2\,H_2O \longrightarrow Mg(OH)_2 + 2\,CH_3OH$$

Clean dry magnesium (1 g.) and resublimed iodine (0.1 g.) were placed in a 500 ml. R.B. Pyrex flask fitted with a double surface condenser. Methanol (12 - 15 ml.) was added and the mixture warmed on a water bath until the iodine reacted and hydrogen was evolved. A further quantity of methanol (200 ml.) was added and refluxed for thirty minutes. The product was then distilled through a 60 cm. fractionating column, filled with glass helices and heated to 64 ^{o}C, the first 10 ml. of distillate being rejected. The rate of distillation was about 2 ml. per minute, and care was taken to exclude moisture from the air.

The dried methanol was then degassed by pumping and distilled under vacuum at room temperature (c.f. formic acid). It was stored at -196 ^{o}C using a liquid nitrogen bath.

Before using the methanol in a run, it was degassed for one minute by pumping while it was melting.

Procedure for each run

The procedure for the decomposition of methanol was in every respect similar to that for the formic acid decomposition, the same static system being used.

The methanol decomposition was investigated with the same alloys as were used for the decomposition of formic acid. A new catalyst, Catalyst II, was included. The decomposition was also carried out on the pure metals.

In general the reaction was followed to between 50 and 70 percent decomposition and in a few cases to completion.

Kinetics of the Decomposition

The decompositions were carried out at temperatures ranging from 140 to 330 °C, and at two different initial pressures, these being approximately 25 and 12 mm. Hg. Blank runs in the absence of catalyst showed that the walls of the reaction vessel did not catalyse the decomposition at 400 °C.

The methanol reaction was not zero order. Initially the reaction was very fast but was soon inhibited by one or both of the products and a very noticable retardation occurred. This effect was observed in varying degrees for all the catalysts used. Although there was great inhibition by the products of the reaction, no falling off in activity of the catalysts was observed provided they were degassed by pumping down to 10^{-5} mm. Hg before proceeding with a further decomposition.

Initial rates were obtained for the decomposition by taking the rate for the first 2.5 and the first 5 percent of the reaction from the pressure increase - time curves.

An estimate of the order of the reaction was obtained from the initial rates at different initial pressures using the following,

$$\frac{\text{Rate 1}}{\text{Rate 2}} = \left(\frac{P_1}{P_2}\right)^n$$

The order of the reaction was not constant. The values obtained varied from 0.35 to 0.70 in a random manner with the different catalysts, an average value being ca. 0.50 - 0.55.

Comparative values of rate constants for the complete reaction were obtained from an expression derived from the Langmuir adsorption isotherm, using the general expression for methanol coverage assuming that product molecules also occupy part of the surface.

The reaction was assumed to follow the equation,

$$CH_3OH \longrightarrow CO + 2\,H_2$$

whence,

$$\theta_M = \frac{k_M P_M}{1 + k_M P_M + k_{H_2} P_{H_2} + k_{CO} P_{CO}}$$

$$-\frac{dP_M}{dt} = \frac{k\, k_M P_M}{1 + k_M P_M + k_{H_2} P_{H_2} + k_{CO} P_{CO}}$$

where P_M = pressure of methanol = $P_o - 0.5\Delta P$

P_{H_2} = pressure of hydrogen = ΔP

P_{CO} = pressure of carbon monoxide = $0.5\Delta P$

P_o = initial pressure

ΔP = increase in pressure

k_M, k_{H_2}, and k_{CO} are constants for methanol, hydrogen, and carbon monoxide respectively.

On integration the following is obtained ,

$$\frac{1}{t} \ln \frac{P_o}{P_o - 0.5\,\Delta P} = \frac{\Delta P}{t} \frac{k_{H_2} + 0.5\,k_{CO} - 0.5\,k_M}{1 + 2k_{H_2}P_o + k_{CO}P_o} + \frac{k\,k_M}{1 + 2k_{H_2}P_o + k_{CO}P_o} \qquad (1)$$

A plot of $\frac{1}{t} \ln \frac{P_o}{P_o - 0.5\,\Delta P}$ against $\frac{\Delta P}{t}$ gives a straight line whose intercept is a measure of the rate. The rates at different temperatures for a given value of P_o can be compared on the assumption that these constants do not vary much with temperature.

The above plot was found to hold for the decomposition of methanol on all the alloys used and was valid for at least fifty percent and in some cases for more than ninety percent of the reaction.

Other expressions deduced from the Langmuir isotherm approach involving the simplifying assumptions that,

$$\theta_M = \frac{k_M P_M}{1 + k_M P_M + k_P P_P} \quad \text{or} \quad \theta_M = \frac{k_M P_M}{k_M P_M + k_P P_P} \quad \text{or} \quad \theta_M = \frac{k_M P_M}{1 + k_{CO} P_{CO}}$$

where k_P = constant for the products

P_P = pressure of the products = $1.5\,\Delta P$

lead respectively to equations (2) , (3) and (4) .

$$\frac{1}{t} \ln \frac{P_o}{P_o - 0.5\,\Delta P} = \frac{\Delta P}{t} \frac{3k_P - k_M}{1 + 6k_P P_o + 2k_M P_o} + \frac{2\,k\,k_M}{1 + 6k_P P_o + 2k_M P_o} \qquad (2)$$

$$\frac{1}{t} \ln \frac{P_o}{P_o - 0.5\,\Delta P} = \frac{\Delta P}{t} \frac{3k_P - k_M}{P_o(6k_P - k_M)} + \frac{2\,k\,k_M}{P_o(6k_P - k_M)} \qquad (3)$$

$$\frac{1}{t} \ln \frac{P_o}{P_o - 0.5\,\Delta P} = \frac{\Delta P}{t} \frac{k_{CO}}{2k_{CO}P_o + 1} + \frac{k\,k_M}{k_{CO}P_o + 1} \qquad (4)$$

These expressions are of a similar type to (1) and again involve plotting $\frac{1}{t} \ln \frac{P_o}{P_o - 0.5\,\Delta P}$ against $\frac{\Delta P}{t}$.

The constant term in each of these integrated equations accounts for the dependence of the rate on the initial methanol pressure as does the constant in equation (1). The inverse proportionality of initial pressure with slope and intercept in the above expressions is apparent in the experimental plots.

The plots obtained for any of the four equations will therefore be identical, and so the expressions are indistinguishable from each other. Expression (4) is the integrated form of the Langmuir isotherm used by Darby and Kemball [51] for the decomposition of methanol over a Fischer-Tropsch cobalt catalyst.

If the products are not considered in the Langmuir adsorption isotherm, then the following is obtained ,

$$\theta_M = \frac{k_M P_M}{1 + k_M P_M} \qquad -\frac{dP}{dt} = \frac{k\,k_M P_M}{1 + k_M P_M}$$

which on integration gives ,

$$\frac{1}{t} \ln \frac{P_o}{P_o - 0.5\,\Delta P} = -\frac{\Delta P\, k_M}{t} + 2\,k\,k_M \qquad (5)$$

This again involves plotting $\frac{1}{t} \ln \frac{P_o}{P_o - 0.5\,\Delta P}$ against $\frac{\Delta P}{t}$ but the slope would have to be negative if k_M is positive. The slope was always positive therefore this expression cannot be valid. This expression also fails to account for the dependence on initial pressure of the slope and intercept /

/ of the experimental plots.

Arrhenius plots were obtained both from the initial rates and from the values of the rate constants derived from the Langmuir isotherm approach.

Results of the Methanol Decomposition

TABLE 7

In Table 7 a selection of the kinetic measurements is given for the decomposition of methanol on copper, nickel and an alloy containing 63.8 atom percent copper.

These show the conversion as a function of time at a fixed temperature for the different initial pressures of methanol.

The accompanying graphs , (Graphs 12, 14, and 16), show the rapid fall in rate as the reaction proceeds, and also that the rate is dependent on the initial methanol pressure.

The table also shows the functions required for a plot of the equation (1) derived from the Langmuir adsorption isotherm. The corresponding graphs , (Graphs 13, 15, and 17), show the linear plots obtained.

TABLE 7

Catalyst I 100 percent Nickel, Weight used = 2.7 g. Surface Area = 3 m^2

Bourdon Gauge factor = 7.8 Temperature = 180 °C

Initial Pressure P_o (scale divisions)		204			106		
Time t (minutes)	ΔP	$\frac{\Delta P}{t}$	$\frac{10^4}{t} \log \frac{P_o}{P_o - 0.5\,\Delta P}$		ΔP	$\frac{\Delta P}{t}$	$\frac{10^4}{t} \log \frac{P_o}{P_o - 0.5\,\Delta P}$
0.25	25	100	916		16	64	1364
0.5	35	70	778		24	48	1044
0.75	43	57.3	644				
1	50	50	567		33	33	735
2	64	32	371		43	21.5	492
3	75	25	285		51	17	398
4	84	21	250		57	14.3	340
6	97	16.2	197		67	11.2	275
8	108	13.5	167		73	9.1	229
10	117	11.7	147		78	7.8	199
15	134	9	115		89	6.0	157
20	147	7.4	97		97.5	4.9	134
30	167	5.5	76		110	3.7	106
45	191	4.3	61				

Catalyst IX 63.8 percent Copper, Weight used = 4.0 g. Surface Area = 2.3 m^2.

Bourdon Gauge factor = 7.8 Temperature = 200 °C

Initial Pressure P_o		211			110		
0.5	19	38	400		15	30	614
1	29	29	309		22	22	458
2	43	21.5	233		32	16	342
3	54	18	198		40	13.3	291
4	63	15.8	176		46	11.5	255
6	79	13.2	150		56.5	9.4	215
8	92	11.5	134		65	8.1	190
10	103	10.3	121		73	7.3	175
15	127	8.5	104		87.5	5.9	147
20	146	7.3	92		99.5	5.0	133
30	177	5.9	79		118.5	4.0	112

GRAPH 12

Cat. 1 100% Ni

Temp. 180°C

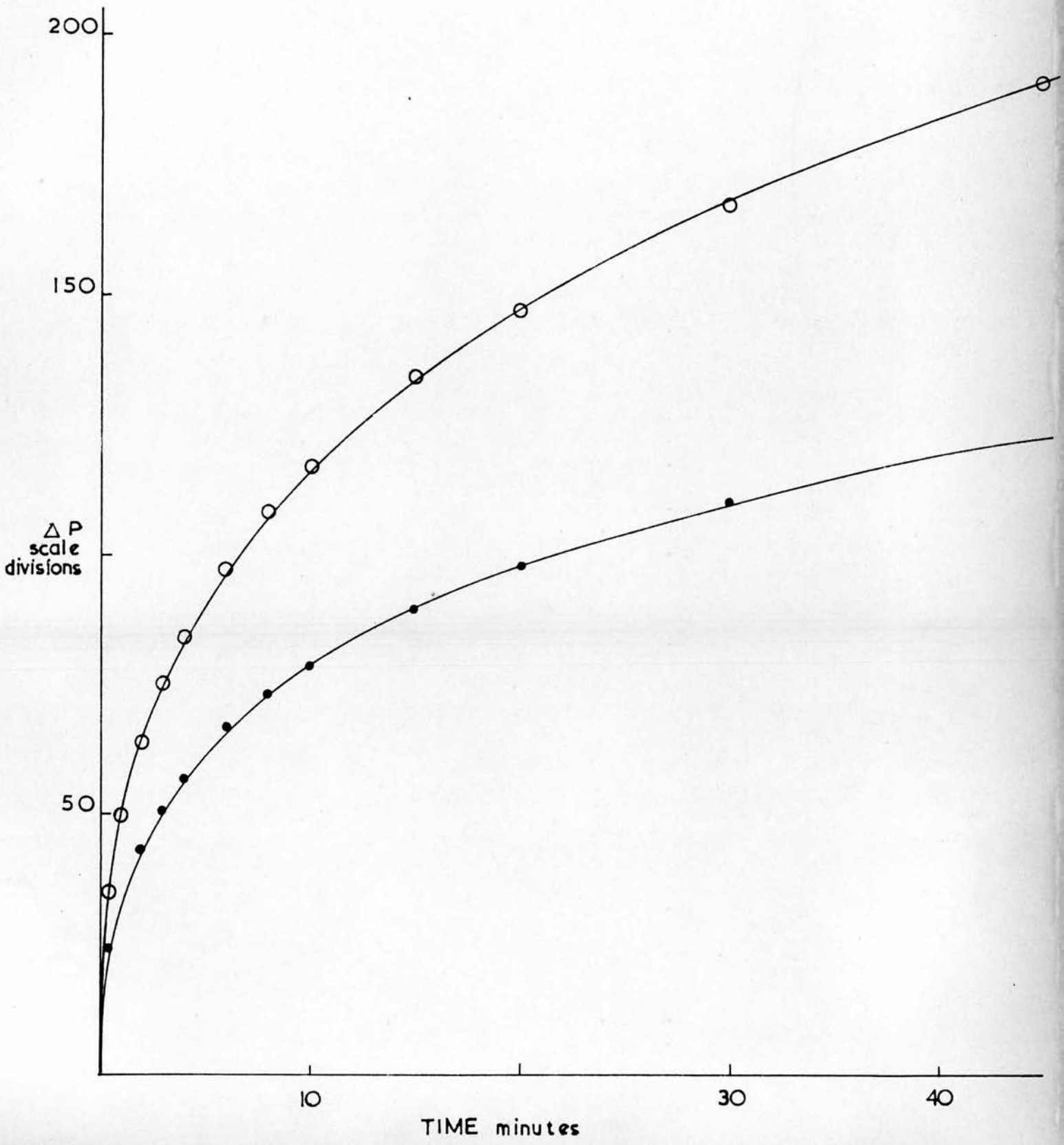

GRAPH 13

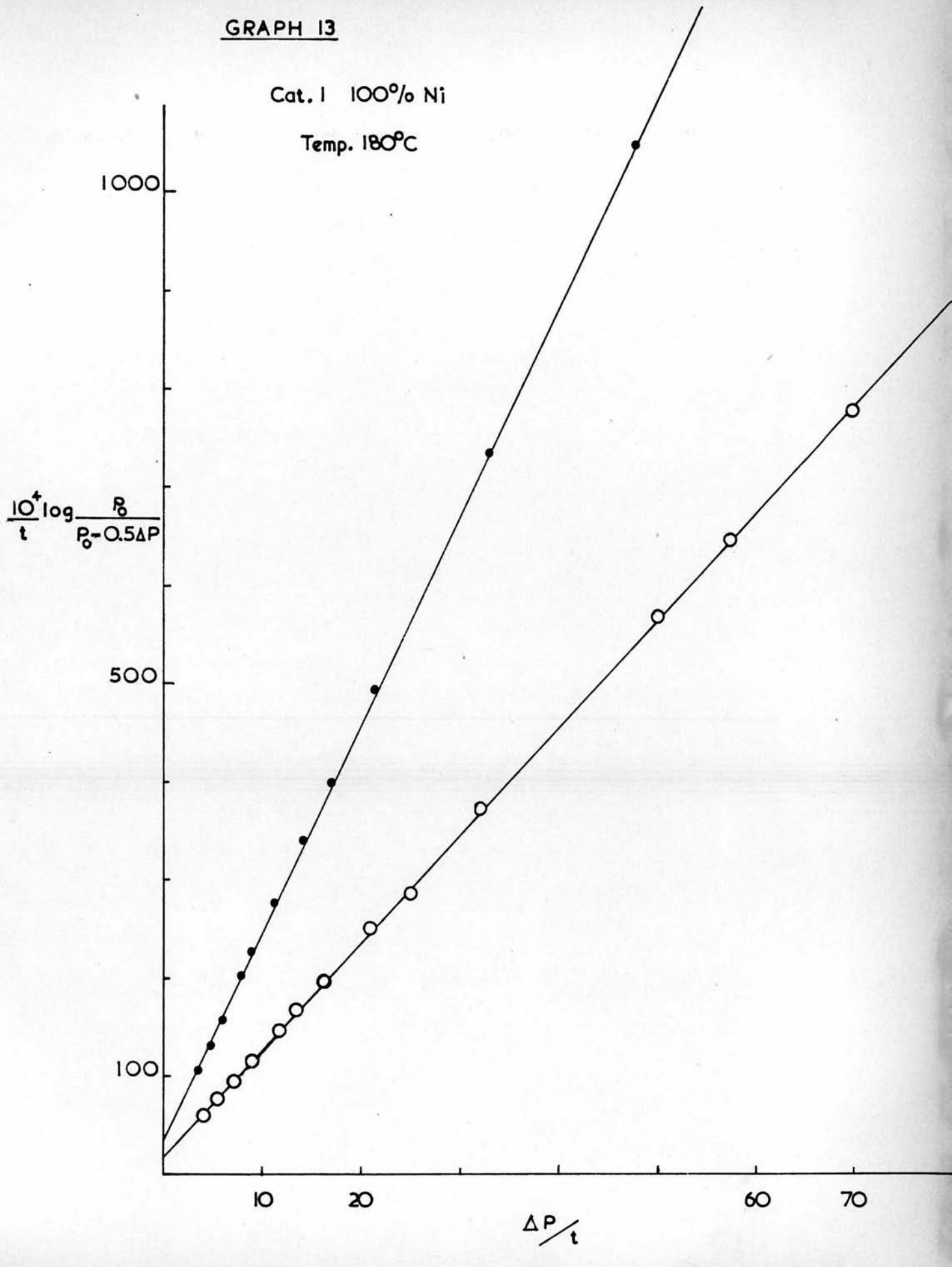
Cat. 1 100% Ni
Temp. 180°C
1000
500
100
$\frac{10^4}{t} \log \frac{P_0}{P_0 - 0.5\Delta P}$
10
20
60
70
$\Delta P / t$

GRAPH 14

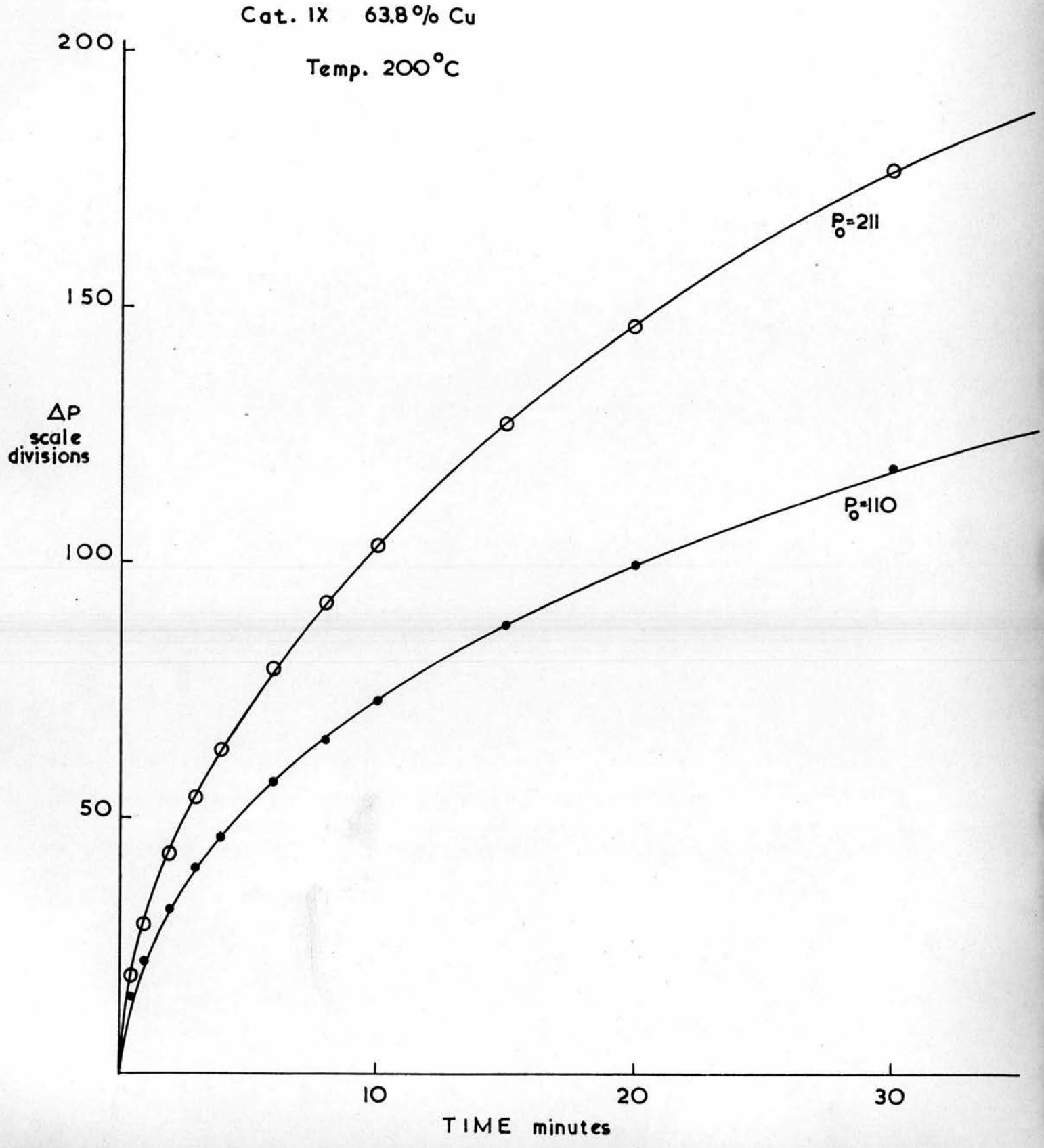
Cat. IX 63.8% Cu
Temp. 200°C
200
150
100
50
ΔP
scale
divisions
P_o=211
P_o=110
10
20
30
TIME minutes

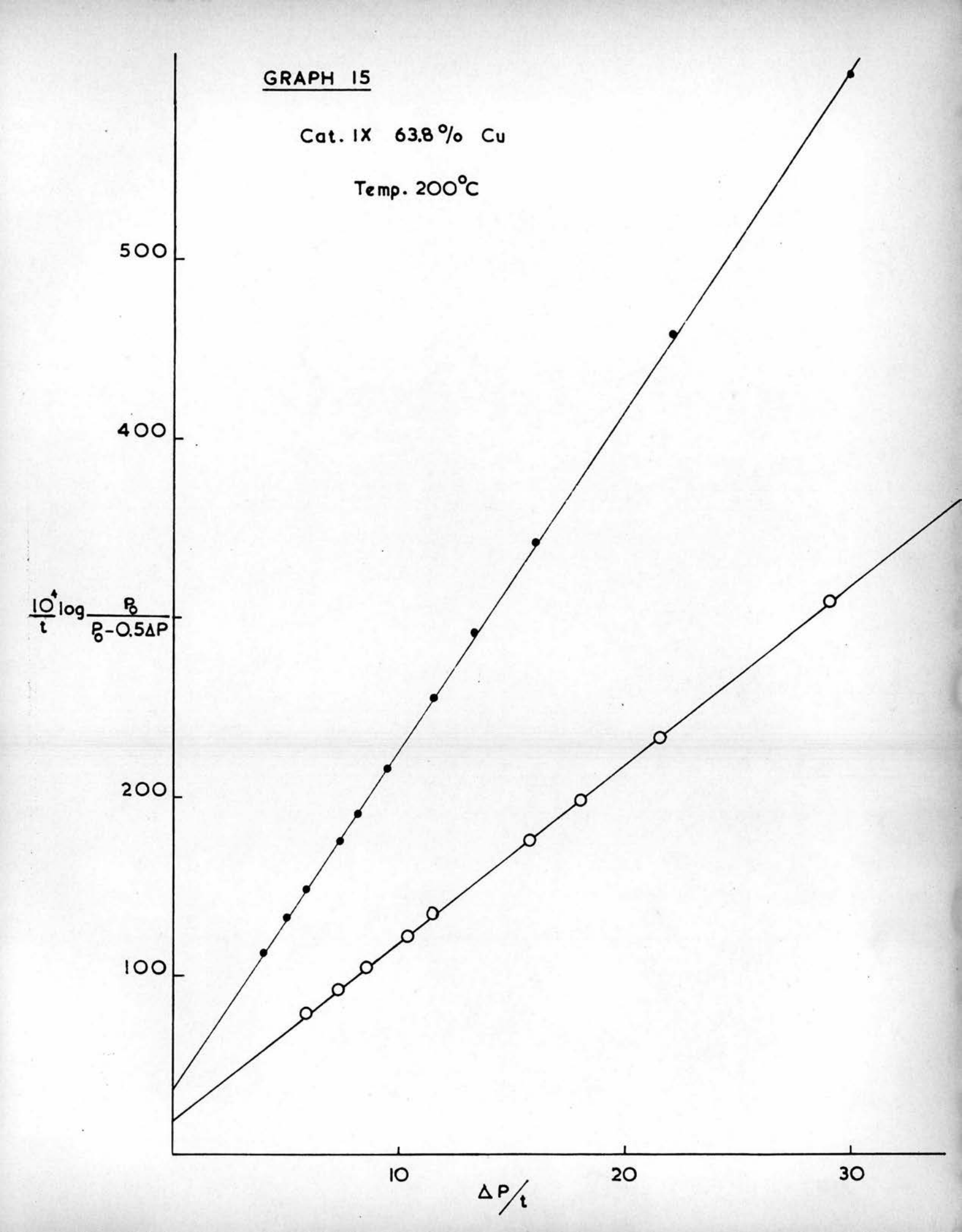
GRAPH 15
Cat. IX 63.8 % Cu
Temp. 200°C
500
400
200
100
$\frac{10^4}{t}\log\frac{P_0}{P_0-0.5\Delta P}$
10
20
30
$\Delta P/t$

TABLE 7 contd.

Catalyst XV 100 percent Copper, Weight used = 3.0 g. Surface Area = 0.75 m^2.

Bourdon Gauge factor = 8.3 Temperature = 280 °C

Initial Pressure P_o (scale divisions)	210			104		
Time t (minutes)	ΔP	$\frac{\Delta P}{t}$	$\frac{10^4}{t} \log \frac{P_o}{P_o - 0.5\,\Delta P}$	ΔP	$\frac{\Delta P}{t}$	$\frac{10^4}{t} \log \frac{P_o}{P_o - 0.5\,\Delta P}$
1	4.5	4.5	46.0	2.5	2.5	52.5
2	8	4.0	41.8	4.5	2.25	47.7
4	14	3.5	36.8	8.5	2.13	45.3
6	19.5	3.3	34.4	11.5	1.92	41.2
8	23.5	2.9	31.3	14.5	1.81	39.2
10	27	2.7	28.9	16.5	1.65	35.9
15	34.5	2.3	24.8	21.5	1.43	31.6
20	40.5	2.0	22.0	26.0	1.30	29.0
30	51	1.7	18.7	32.5	1.08	24.6
45	64	1.4	16.0	40.5	0.90	21.0
60	75.5	1.3	14.3	48	0.80	19.0
80	89	1.1	12.9			

GRAPH 16

Cat. XV 100% Cu

Temp. 280°C

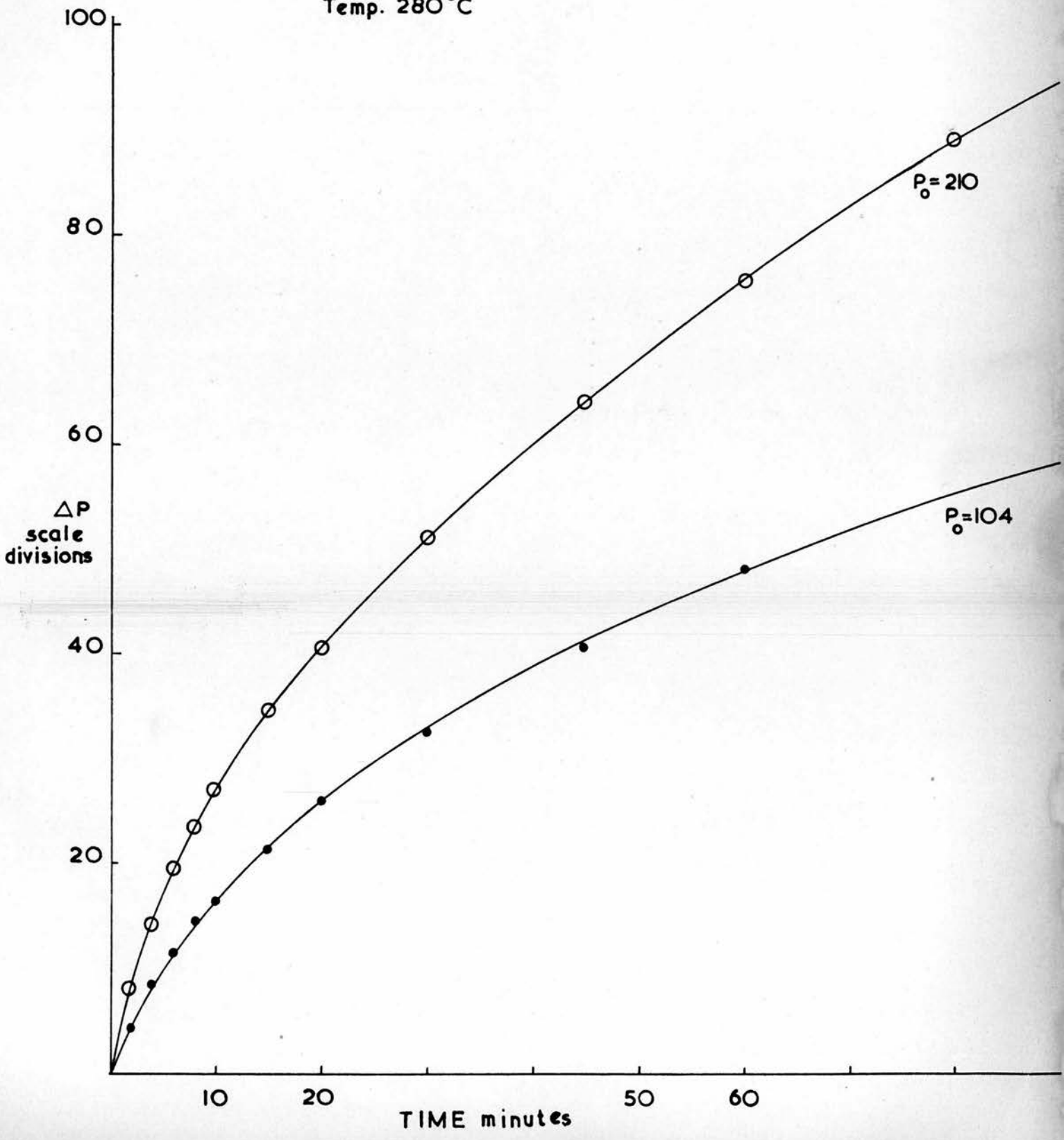

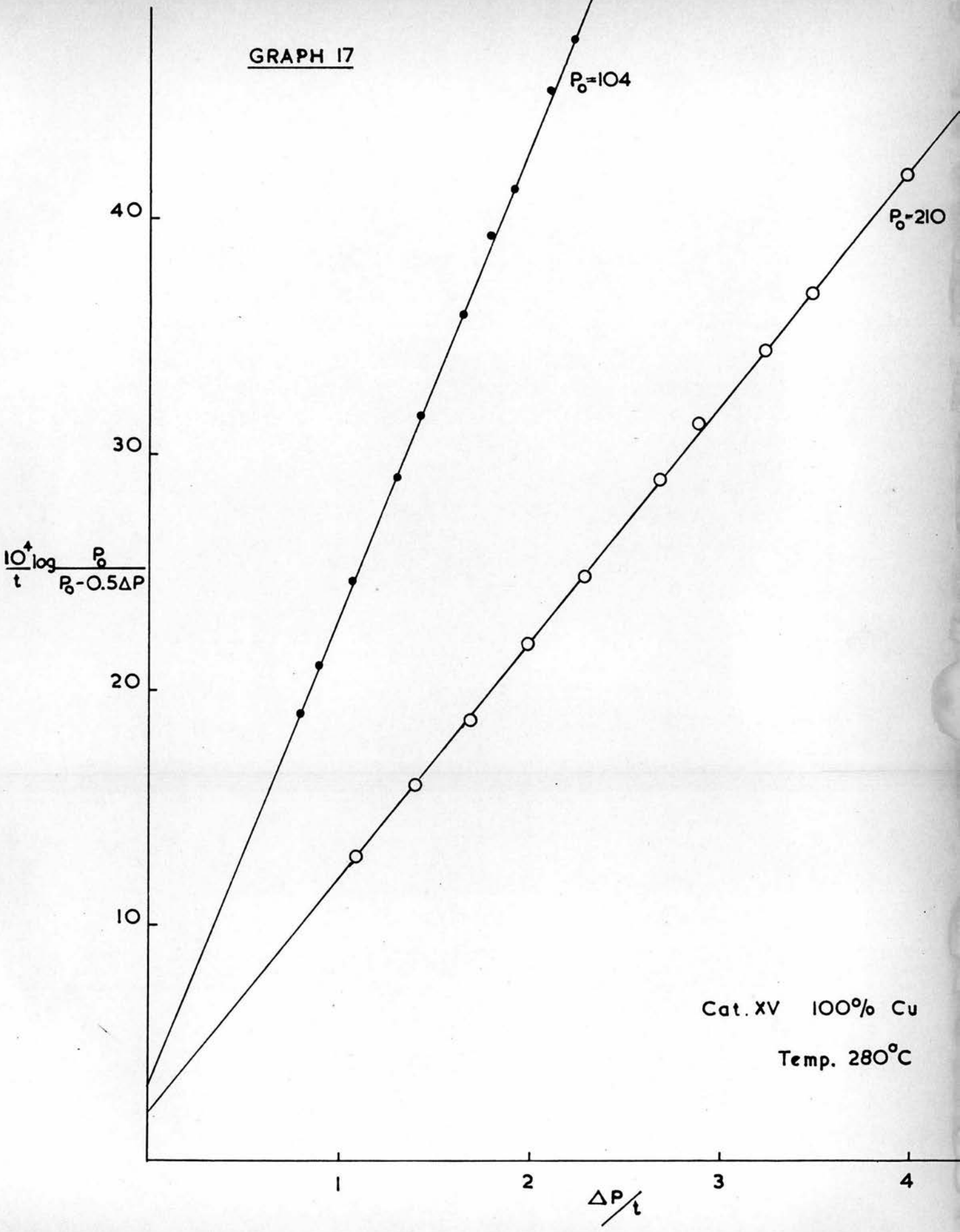
GRAPH 17
P_0=104
P_0=210
40
30
20
10
$\frac{10^4}{t}\log\frac{P_0}{P_0-0.5\Delta P}$
1
2
3
4
$\Delta P/t$
Cat. XV 100% Cu
Temp. 280°C

TABLE 8

For comparative purposes, the initial rates for the first 2.5 and the first 5 percent of the decomposition at two different initial pressures have been given in Table 8.

The rates have been calculated, as for the formic acid reaction, in molecules $site^{-1}$ $second^{-1}$.

In some cases, 'arbitrary' values of the rate constant for the reaction are also given. These values are derived from the intercepts of the linear plots of the expressions derived from the Langmuir adsorption isotherm. No great confidence is placed in these arbitrary values in view of the assumption regarding k_M , k_P etc.

Arbitrary rate constants are designated by 'Langmuir Constants'.

TABLE 8

Temperature °C	Initial Pressure P_o mm. Hg	Rate mols. site^{-1} sec.$^{-1}$ x 10^4 2.5 %	Rate mols. site^{-1} sec.$^{-1}$ x 10^4 5 %	'Langmuir Constants'
Catalyst I	100 percent Nickel			
140	25.6	7.4	2.3	5
	13.2	6.6	4.5	15
150	26.9	17.9	7.6	15
	13.2	14.7	10.7	35
160	26.7	25.5	14.7	30
	13.6	23.1	19.9	80
170	25.0	41.9	35.8	50
	14.3	24.9	23.3	120
180	26.2	98.7	81.2	150
	13.6	62.2	54.0	350
190	26.2	141.0	127.0	300
	13.1	81.8	75.8	600
200	26.4	167.0	150.0	400
	13.6	153.0	138.0	800
Catalyst II	13.0 percent Copper			
150	24.4	20.1	7.8	10
	11.6	11.2	6.1	20
160	24.4	22.3	10.4	15
	12.1	12.5	8.4	35
170	24.4	45.1	25.8	40
	12.1	30.4	21.3	60
180	25.3	78.4	65.4	50
	12.1	40.5	35.5	150
190	24.9	151.0	125.0	250
	11.2	67.5	60.5	450
200	24.4	160.0	143.0	400
	11.6	114.0	108.0	700

TABLE 8 contd

Temperature °C	Initial Pressure P_o mm. Hg	Rate mols. site^{-1} sec.$^{-1}$ $\times 10^4$ 2.5 %	Rate mols. site^{-1} sec.$^{-1}$ $\times 10^4$ 5 %	'Langmuir Constants'
Catalyst III	20.1 percent Copper			
140	24.4	6.4	2.1	
	12.4	4.7	2.5	
150	24.2	9.5	5.0	
	12.5	12.4	8.0	
160	24.5	25.3	13.0	
	12.4	17.8	15.8	
170	25.4	32.0	22.9	
	11.3	18.2	16.0	
180	24.6	83.0	59.0	
	12.3	50.0	43.7	
190	26.0	118.0	99.2	
	12.3	73.4	69.0	
Catalyst IV	29.3 percent Copper			
180	26.4	8.7	4.8	10
	12.8	5.5	3.5	15
200	26.2	15.2	11.2	50
	13.6	10.2	8.2	90
225	25.1	65.8	54.6	420
	13.7	51.7	42.8	700
250	27.0	82.3	74.7	2200
Catalyst IV	Repeated			
180	24.1	7.1	5.0	
190	24.6	14.6	10.5	
	12.8	13.8	9.2	
200	24.4	17.2	12.8	
	12.5	12.8	11.1	
210	24.6	38.3	24.8	
	12.5	28.5	23.0	
220	25.4	55.0	43.8	
	12.4	38.2	31.9	
230	24.8	95.1	74.4	
	12.1	54.0	45.5	
240	24.1	114.0	87.9	
	11.6	64.8	58.1	

TABLE 8 contd.

Temperature °C	Initial Pressure P_o mm. Hg	Rate mols. site^{-1} sec.$^{-1}$ × 10^4 2.5 %	Rate mols. site^{-1} sec.$^{-1}$ × 10^4 5 %	'Langmuir Constants'
Catalyst VI	49.6 percent Copper			
170	25.3	4.4	2.9	5
180	26.7	8.2	5.3	15
	13.2	5.3	4.1	35
200	27.4	25.5	17.7	90
	13.2	15.7	13.1	150
210	25.4	60.0	56.0	300
	26.0	96.0	68.0	250
225	26.7	119.0	103.0	600
	13.8	96.0	87.0	900
Catalyst IX	63.8 percent Copper			
160	26.2	5.8	3.0	10
	13.6	4.3	3.0	30
170	27.2	7.6	5.5	15
	14.1	7.8	6.0	30
180	27.2	16.2	11.0	30
	13.1	10.7	8.4	80
190	25.9	33.9	24.8	80
	13.6	25.2	17.4	170
200	27.0	39.9	32.7	170
	14.1	34.0	30.3	360
210	27.7	68.7	57.5	400
	13.6	55.7	35.3	650

TABLE 8 contd.

Temperature °C	Initial Pressure P_o mm. Hg	Rate mols. site^{-1} sec.$^{-1}$ × 10^4 2.5 %	Rate mols. site^{-1} sec.$^{-1}$ × 10^4 5 %	'Langmuir Constants'
Catalyst XII	69.2 percent Copper			
140	24.5	2.7	1.2	
	12.2	1.8	1.1	
150	24.6	6.5	3.4	
	12.5	3.4	2.7	
160	25.2	9.3	6.5	
	12.4	9.1	6.9	
170	24.7	18.2	12.9	
	12.0	9.6	8.4	
180	24.6	27.9	22.0	
	12.0	18.5	15.8	
190	23,8	41.9	36.5	
	12.3	38.3	33.6	
200	25.3	131.0	95.3	
	12.4	74.9	66.4	
Catalyst XIII	82.8 percent Copper			
150	27.2	7.2	4.2	15
	12.3	5.3	3.2	30
160	27.2	17.3	12.3	25
	13.3	13.8	11.4	50
170	25.9	25.6	19.6	60
	12.4	22.7	18.9	100
180	27.7	52.4	44.5	100
	12.8	37.8	36.4	250
190	26.2	113.0	94.8	280
	13.6	53.9	47.3	450
200	26.2	138.0	124.0	550
	13.1	92.8	91.6	900
210	22.8	187.0	187.0	1200
	13.1	182.0	182.0	2300

TABLE 8 contd.

Temperature °C	Initial Pressure P_o mm. Hg	Rate mols. site^{-1} sec.$^{-1}$ × 10^4 2.5 %	Rate mols. site^{-1} sec.$^{-1}$ × 10^4 5 %	'Langmuir Constants'
Catalyst XIV	92.6 percent Copper			
190	28.0	4.9	3.0	20
	13.7	2.8	2.1	40
200	25.4	8.7	5.7	60
	13.0	4.9	4.1	130
210	27.0	7.7	6.7	130
	14.1	5.3	4.7	240
220	26.2	8.0	7.8	250
	13.9	6.5	5.9	380
230	27.7	16.3	14.7	500
	13.6	12.7	11.5	810
240	26.2	19.2	17.0	780
	13.6	12.9	12.4	1100
Catalyst XV	100 percent Copper			
240	25.0	1.7	1.1	2
	12.4	0.9	0.8	4
260	23.9	3.6	2.6	6
	13.3	3.3	2.1	8
280	25.3	7.1	5.8	16
	12.5	5.3	4.7	30
300	25.5	17.4	15.2	50
	13.5	10.5	10.1	80
320	26.0	32.7	29.1	150
Catalyst XVA	L00 percent Copper			
250	25.4	8.9	7.9	
	13.6	7.1	6.0	
275	25.9	27.7	19.7	45
	13.2	21.9	18.5	50
300	26.3	83.6	64.6	80
	13.2	56.6	50.7	100
325	25.6	263.0	225.0	200
	13.2	205.0	230.0	250

TABLE 9

In this table the activation energies obtained from Arrhenius plots of the initial (2.5 %) rates for the various catalysts are shown.

The pre-exponential (or A) factor is shown in molecules site^{-1} second^{-1}. Activation energies derived from Arrhenius plots of the 'arbitrary' rate constants are also given.

The variation of activation energy and of activity (given by the rate of decomposition at a fixed temperature) as a function of alloy composition is given on Graphs 18 and 19.

The compensation effect of the pre-exponential factor and the activation energy is shown in Graph 20.

TABLE 9

Catalyst	Atom percent Copper	Activation Energy kcals.mole^{-1}	A mols.site^{-1}sec.$^{-1}$	log A	A.E. from 'Langmuir Constants'
I	0	23.0 ±2.0	8×10^{8}	8.9	32.0 ±2.0
II	13.0	23.0 "	8×10^{8}	8.9	33.0 "
III	20.1	22.5 "	4×10^{8}	8.6	
IV	29.3	22.0 "	3.2×10^{7}	7.5	37.0 "
IVR	29.3	21.0 "	1.3×10^{7}	7.1	
VI	49.6	27.0 "	9.8×10^{9}	9.9	33.5 "
IX	63.8	23.0 "	2.0×10^{8}	8.3	34.5 "
XII	69.2	24.0 "	8.0×10^{8}	8.9	
XIII	82.2	23.0 "	5.0×10^{8}	8.7	30.0 "
XIV	92.6	22.0 "	6.3×10^{6}	6.8	33.5 "
XV	100	24.0 "	3.2×10^{6}	6.5	31.0 "
XVA	100	27.0 "	2.0×10^{8}	8.3	17.0 "

GRAPH 18

METHANOL

Activation Energy / Composition

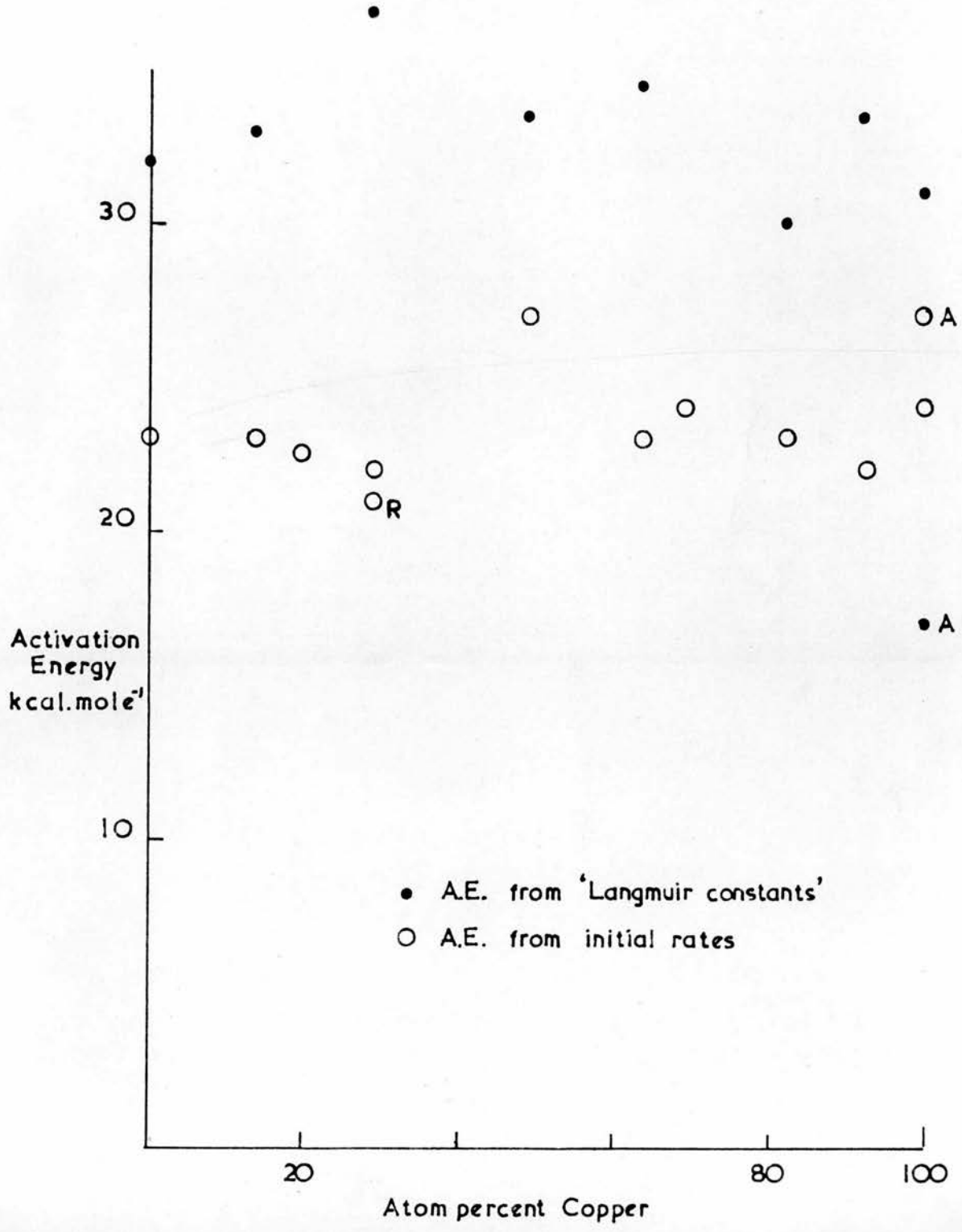

GRAPH 19

METHANOL

Activity Pattern at 200 °C

Rate measured in molecules site^{-1} sec.$^{-1}$

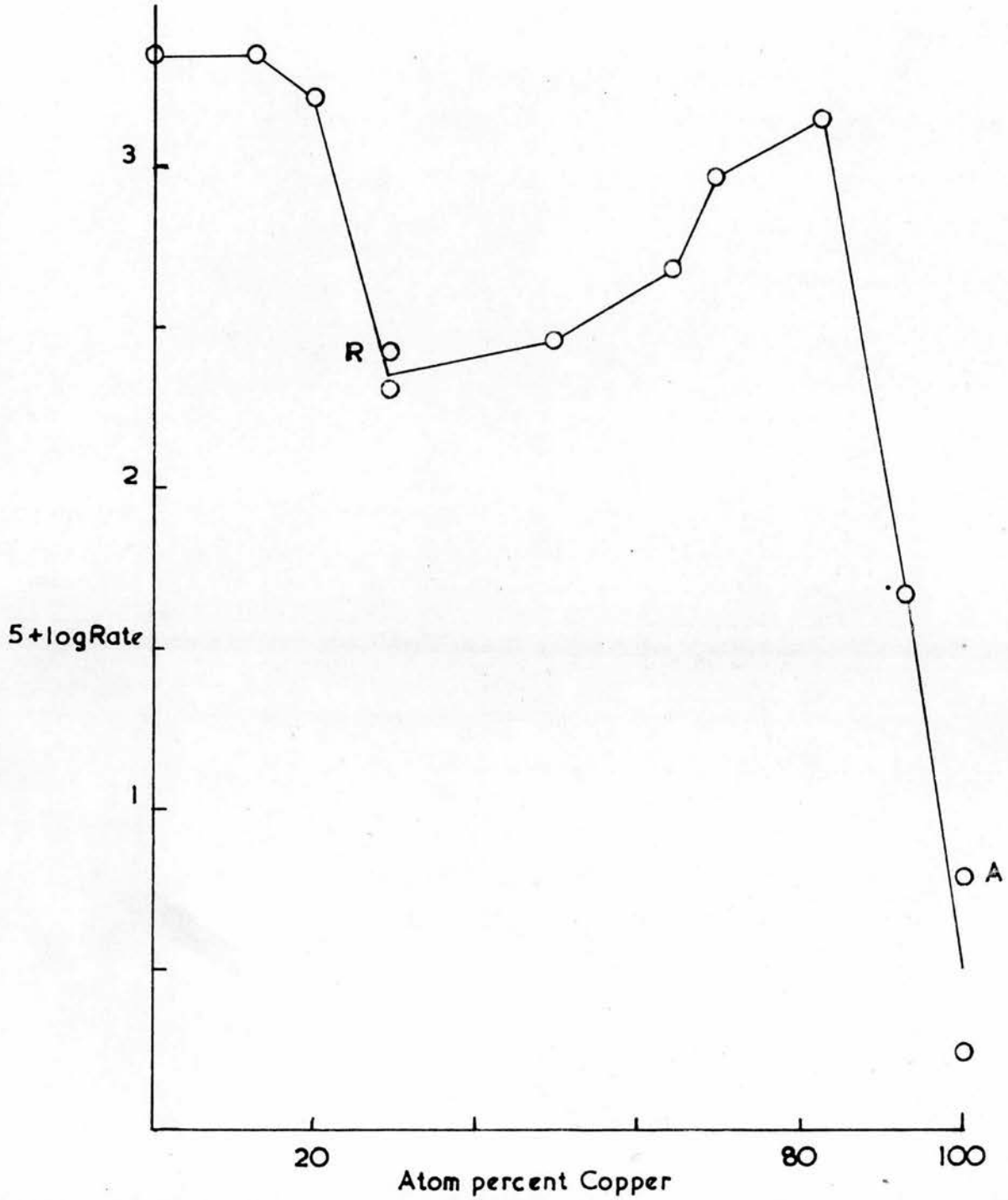

GRAPH 20

METHANOL

Compensation Effect

Numbers represent atom percent copper

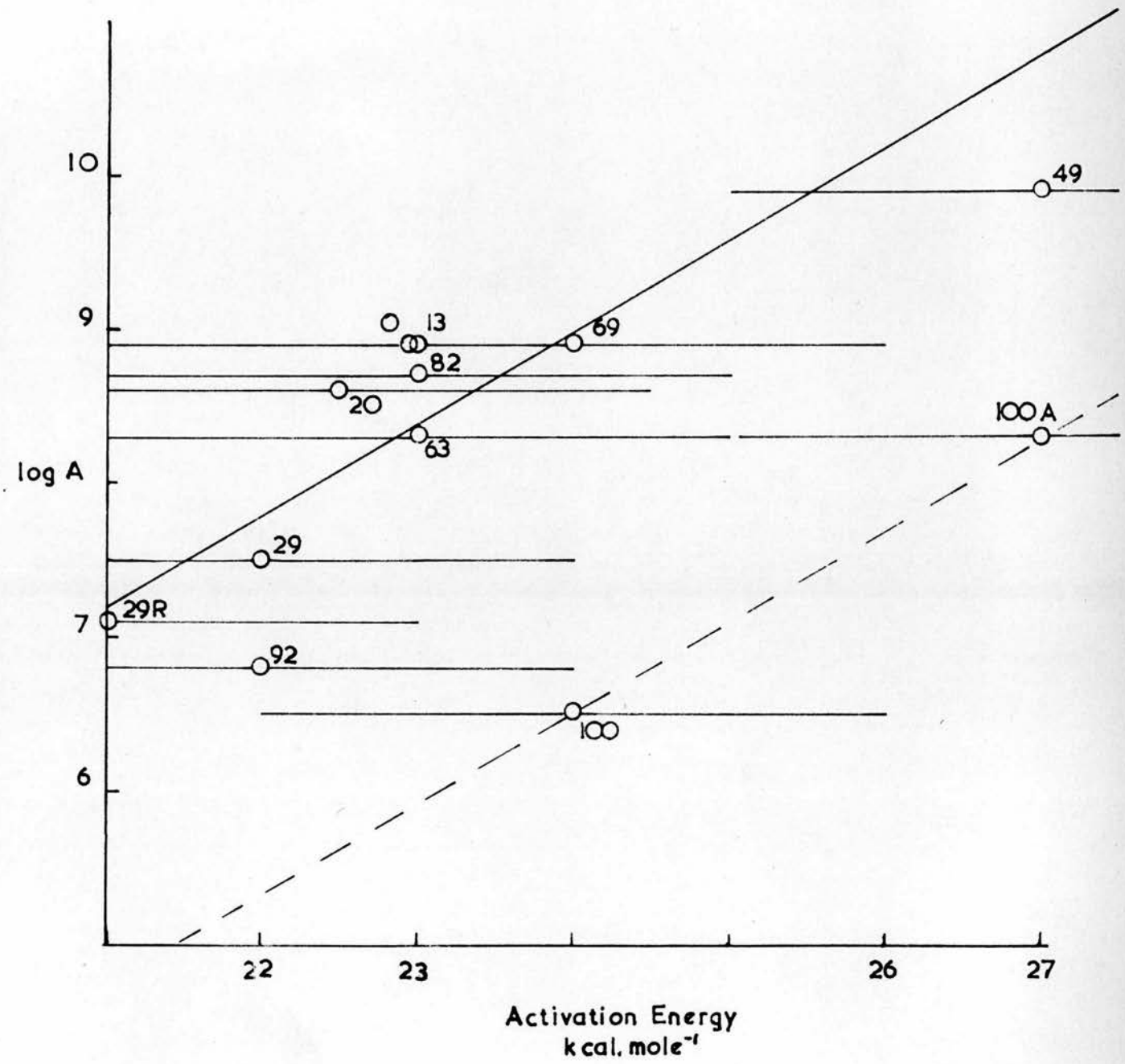

TABLE 10

It has been assumed that the copper and nickel atoms in these alloys retain the same d-character as that given by Pauling [5] for the pure metals. Although this is not consistent with lattice spacing and magnetic results, Hall and Emmett have shown that the correction for this is small,[10]. The percentage d-character for the alloys has therefore been calculated assuming that it changes linearly with composition.

Graph 21 shows the activity patterns obtained when the logarithm of the rate at 200 °C for methanol decomposition on alloys of copper and nickel, is plotted against the valency of the alloy, the percentage d-character, and the product of both these functions.

GRAPH 21

METHANOL

Activity Patterns at 200°C

Rate measured in molecules site^{-1} sec.$^{-1}$

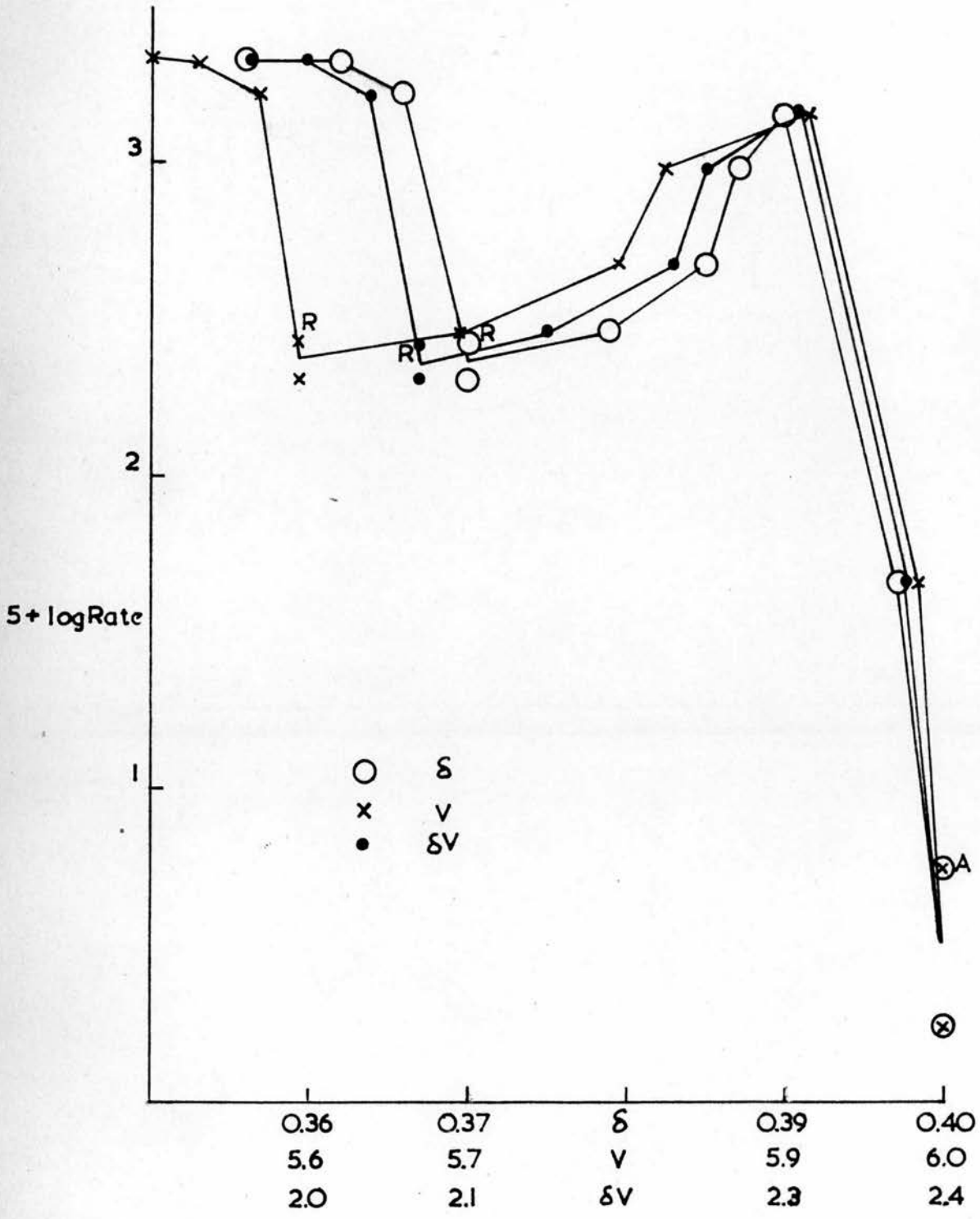

TABLE 10

Catalyst	Atom percent Copper	Valency V	Percentage d-character δ	Vδ	log Rate at 200 °C + 5
I	0	5.500	0.357	1.963	3.34
II	13.0	5.530	0.362	2.002	3.34
III	20.1	5.565	0.366	2.037	3.22
IV	29.3	5.595	0.370	2.070	2.30
IVR	29.3	5.595	0.370	2.070	2.42
VI	49.6	5.695	0.379	2.158	2.46
IX	63.8	5.795	0.385	2.231	2.68
XII	69.2	5.825	0.387	2.254	2.98
XIII	82.2	5.915	0.390	2.307	3.14
XIV	92.6	5.984	0.397	2.376	1.66
XV	100	6.000	0.400	2.400	0.23
XVA	100	6.000	0.400	2.400	0.77

DISCUSSION

Copper and nickel occupy adjacent positions in the Periodic Table. Both have similar atomic radii (1.28 Å ~ 1.24 Å respectively) and have face centred cubic lattice structures. Accordingly they form one continuous series of substitutional solid solutions. A similar and comparable system is that of silver and palladium.

Since the electronic properties of these alloys vary continuously with composition, studies of some of their physical properties will show any change in electronic structure which may occur with change in composition.

Magnetic susceptibility measurements of alloys have been used to indicate the presence of unpaired electrons in the d-band. If the 3d-band of copper and nickel, or the 4d-band of silver-palladium alloys is filled at 60 atom percent copper and silver respectively as predicted by the electron band theory (the valency bond theory of Pauling arrives at the same prediction) then there should be a marked fall in susceptibility at this point.

The saturation magnetic moment measurements of Alder [59] on alloys of copper and nickel extrapolate to zero moment at 60 atom percent copper. This was interpreted by Mott and Jones[6] to indicate the filling of the d-band at 60 atom percent copper on the assumption that the number of electrons per atom in the 4s-band remains constant at 0.6 per atom as for pure nickel. Martin, Ahern and Sucksmith [53] have made similar measurements recently and shown the extrapolated value to be nearer 53 atom percent copper. Wohlfarth [54] on the other hand suggests that the number of d-band holes does not become zero until a copper content of 65 atom percent is reached.

Weiss and de Marco [55] have made a direct determination of the number of electrons in the copper d-band and have shown it to be 9.8 + or - 0.2 per atom.

An examination of the palladium-silver system by Wohlfarth [54] indicates that the number of unoccupied states in the 4d-band should drop to zero at about the same point as in the nickel-copper system, that is about 60 atom percent silver.

Examination of the palladium-silver system in this way by Svensson [56] showed the exact behaviour expected if the d-band is completely filled at about 60 atom percent silver. Kaufmann and Starr [40] measured the magnetic susceptibilities of the alloys of copper and nickel. Their results show that alloys containing as little as 5 atom percent nickel are paramagnetic. From this it appears that even at copper contents considerably higher than 60 atom percent there are d-band vacancies. To account for this the suggestion has been made that the alloys are inhomogeneous and 'islands' of nickel exist in a matrix of copper. This seems unlikely for several reasons [36]. Copper rich alloys have a resistance higher than that which would be given by a matrix of nearly pure copper with 'islands' of nickel. The thermoelectric properties are considerably different from those of the palladium-silver system and the high values found for the electronic specific heats of alloys of high copper content imply the existance of d-band holes.

Both the palladium-silver and nickel-copper alloy systems deviate from Vegard's Law which states that the lattice spacing should vary linearly with composition. An investigation of the lattice spacings of both systems by Coles [35] showed that for the palladium-silver system a marked change in slope of the lattice-spacing / composition curve was apparent near 60 atom percent silver,

/ where other properties of this system suggest that the d-band has become fully occupied. The similar discontinuity in slope at 66 atom percent copper reported by Owen and Pickup [7] for the copper-nickel system has been quoted to support the view that the d-band in this system is completely full at this point. Coles however found for this system a change in slope at 33 atom percent copper : this effect he ascribes to the Curie point and not to the filling of the d-band.

It is therefore evident that there are marked differences between the palladium-silver and the nickel-copper systems. The electron band theory adequately explains the experimental physical data on palladium-silver alloys but fails to explain the paramagnetic properties of the copper rich nickel-copper alloys, (if all the d-band states are occupied diamagnetism is to be expected as shown by pure copper).

Several suggestions and models to explain the deviations of this system from the collective band treatment have been put forward by Coles by none however are totally satisfactory.

Prehaps the recent figure of Weiss and de Marco [55] for the average number of electrons in the 3d-band of copper of 9.8 + or - 0.2 suggests that some vacancies do exist in the copper d-band. If this were so then some of the physical properties of the solid solutions could be more easily explained.

In spite of these deviations in physical properties from that predicted by theory the copper-nickel system is still of great interest catalytically.

Alloys of copper and nickel for catalytic investigations are often prepared chemically rather than by combining the molten metals.

Because of this it is advisable to establish whether or not the chemically prepared alloys possess the same physical properties (relating to their electronic rather than their geometric structure) as their annealed or quenched counterparts.

Magnetic susceptibility and X-ray diffraction measurements were carried out on the alloys prepared for this work. It was established that the alloy catalysts used followed the same linear relationships in a lattice spacing / composition plot as those of Owen and Pickup [7]. A maximum deviation from homogeneity of 3 percent was claimed by Hall and Alexander [30] who prepared copper-nickel alloy catalysts in the same way as in the present work, but Sabatha and Selwood [57] from magnetic measurements have shown that some of the alloys could deviate from homogeneity by twice this amount. As stated previously the magnetic susceptibility measurements are in agreement with the literature. These show considerable paramagnetism for alloys of copper content greater than 60 atom percent indicating that d-band vacancies still persist at copper contents greater than 60 atom percent copper.

The catalysts prepared for this investigation are then, as far as can be ascertained, homogeneous solid solutions of copper and nickel exhibiting the same properties as alloys prepared by more direct methods and have a surface area large enough to make them suitable for catalysis.

If therefore a reaction on the surface takes place in the formation of a covalently or ionically bound activated complex, the activity pattern shown by alloys of copper and nickel for such a reaction should conform to a modified form of those idealised patterns outlined by Bond and Mann [8] since d-band vacancies appear to exist up to at least 95 atom percent copper.

If an electronic effect is observed, an activity pattern conforming to one of the following should be apparent.

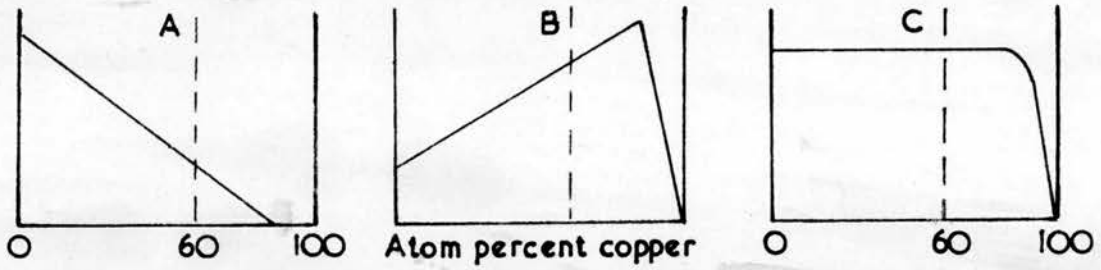

These diagrams are similar to those given by Bond and Mann but their critical composition has been displaced to copper contents some 20 - 30 atom percent higher. These theoretical activity patterns for the copper-nickel system have been supported experimentally by the investigation of several reactions on these alloys.

Pattern A is followed by the hydrogenation of cinnamic acid on kieselguhr supported alloys at room temperature [58] and by the hydrogenation of acetylene on powders at 50 °C [8].

Hydrogenation of acetylene at 200 °C however conforms to pattern B, [8] as does the hydrogenation of benzene on powders at 162 °C [12] and 190 °C [59].

Pattern C is shown by the para-hydrogen conversion on foils at 496 °C [60] and on powders at -196 °C [61]. Both the hydrogenation of cinnamic acid on powders at 20°C [58] and the hydrogenation of ethylene on foils at 500 °C [13] also conform to this activity - composition pattern.

The explanation put forward to account for the activity of alloys of copper contents above the normal critical composition (> 60 atom percent copper) is that further d-band vacancies can be created by thermal excitation.

This does not seem likely since Pugh, Ryan and Smoluchowski [39] have shown that the magnetic susceptibilities of alloys containing more than about 73 atom percent copper are temperature independent. Alloys of copper content less than this show an increase in susceptibility at lower temperatures which is described generally by a 1 / T law.

When attempting to assess the catalytic activities of sustances using a test reaction it is desirable that either the mechanism of the reaction is already clearly understood or that during investigation an effort is made to elucidate the mechanism.

Unfortunately the decomposition of formic acid on metals is more complicated in its mechanism than it would appear at first sight. Schwab [19,62] from investigations of this decomposition on various alloys suggested that the mechanism involved an electron transfer to the metal.

$$HCOOH \longrightarrow HCOOH^{+} + e$$

$$HCOOH^{+} \longrightarrow CO_2^{+} + H_2$$

$$CO_2^{+} + e \longrightarrow CO_2$$

This view was also held by Dowden and Reynolds [9] from similar studies of the decomposition.

The mechanism proposed by Eley and Luetic [18] does not require an electron transfer to the catalyst but suggests that the activated complex is formed by the setting up of a surface dipole between the bulk metal and the hydrogen atoms of the formic acid molecule.

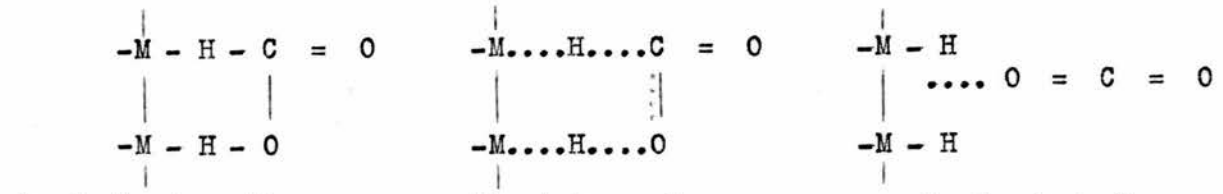

physical adsorption activated complex chemisorbed H

It is important to point out that these mechanisms were proposed only as a result of trends observed in activity patterns and not by direct investigation of the catalyst surface during adsorption.

Recently, however, a number of workers have tried to ascertain the mechanism by investigation of the catalyst surface during adsorption of formic acid.

Rienacker and Hansen [63,64] found that the electrical conductivity of hydrogen covered nickel films decreased on adsorption of formic acid at 200 °C. This, they suggested, indicated the dissociation of the formic acid molecule to a formate ion and a proton, the latter reacting with preadsorbed hydrogen to form molecular hydrogen. In this way the reaction proceeds by the transfer of an electron from the catalyst to the adsorbate.

Similar measurements of the resistance of a nickel film were made by Suhrmann and Wedler [65,24] at room temperature. They found an immediate decrease in resistance of the film on adsorption of formic acid, followed by a gradual increase in resistance. The latter, they concluded, was due to chemisorbed carbon monoxide because this gas was the only product of the decomposition which gave an increase in the resistance of the film. Their results suggest that the decomposition involves the same electron transfer process as proposed by Schwab [19], but with carbon monoxide and water instead of carbon dioxide and hydrogen as products.

It may be that at 200 °C the rate of decomposition was so fast that Rienacker and Hansen only noticed the increase in resistance due to the rapid formation of carbon monoxide on the surface and failed to detect the initial decrease in resistance reported by Suhrmann and Wedler.

Infra - red studies of chemisorbed formic acid on silica supported metals have been of value in assessing which species are present on the catalyst surface. Hirota, Kuwata and Nakai [22] reported absorption bands at approximately 1570 and 1360 cm^{-1} when formic acid was adsorbed on silica supported metals. They pointed out the similarity of the spectra to those of metal formates but did not ascribe any charge to the adsorbed species. Fahrenfort et al [20,66] substantiated this work and from it concluded that the decomposition of formic acid took place via the formation of a metal formate involving an electron transfer from the metal to the adsorbate. This similarity in spectra between the adsorbed species and the formate ion means that the species and the ion have similar symmetrical structures, but gives no indication of the charge which they may carry.

The spectrum obtained by Eischens and Plisken [67] of formic acid adsorbed on nickel-silica at -60 °C was dissimilar to that obtained by the Dutch and Japanese workers, and they have attributed their spectrum to covalently chemisorbed formic acid. At room temperature, the -60 °C spectrum was replaced by one characteristic of the linear and bridged structures of carbon monoxide. The latter spectrum was also obtained from mixtures of carbon dioxide and hydrogen. Eischens and Plisken also investigated the infra - red spectra of deuterated formic acids on nickel silica.

GRAPH 22

FORMIC ACID

Normalised Activity Patterns

Rate in arbitrary units

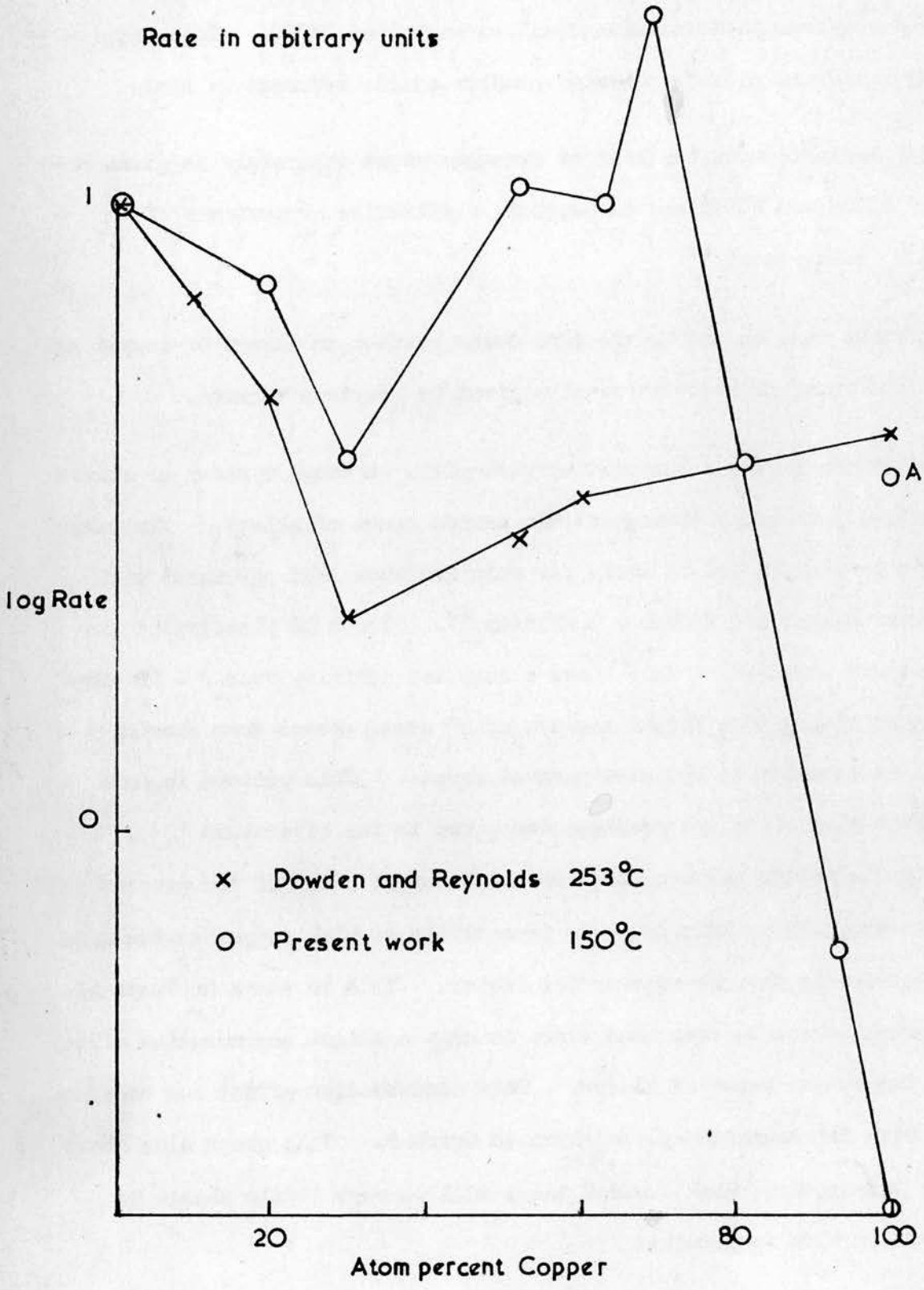

They found that the spectrum from HCOOD was the same as that from HCOOH and the spectrum from DCOOH was identical to that from DCOOD. This suggests that in the formation of the activated complex acidic hydrogen is lost.

Another indication of the loss of hydrogen atoms separately is given when mixtures of HCOOH and HCOOD are decomposed, equilibrium proportions of H_2, HD and D_2 being found [21].

The present work on the formic acid decomposition on alloys of copper and nickel has confirmed many of the results given by previous workers.

The activation energy / composition plot given on Graph 9 shows an almost constant activation energy throughout the entire range of alloys. The values obtained lie between 21 and 27 kcal. per mole and show good agreement with the results of Schwab and Schwab - Agallidis [17]. Graph 10 illustrates the activity pattern obtained. This shows a constant activity from 0 - 70 atom percent copper rising to a slight maximum at 80 atom percent then showing a marked fall in activity to 100 atom percent copper. This pattern is more pronounced but similar to the previous two given in the literature [9, 15]. The normalised activity patterns of Dowden and Reynolds and of the present work are shown in Graph 22. This decrease in activity at high copper contents is due to a decrease in the pre-exponential factor. This is shown in Graph 11. From this graph it can be seen that there is only a slight compensation effect throughout the entire range of alloys. This compensation effect can be seen once again from the Arrhenius plots given in Graph 8. This graph also shows that in the temperature range studied there will be very little change in activity pattern with temperature

Reproducibility of results was very good provided the same catalyst preparation was used. In order to check the reproducibility of results with different catalyst preparations, another catalyst of pure copper was prepared in an identical way to the original. This new catalyst was designated XVA. As can be seen from Table 6 this catalyst was considerably more active than the original preparation (XV) but was less active than all the other catalysts except XIV (92.6 atom percent copper). In spite of this the overall activity or activation energy pattern remains almost unchanged and there seems to be little doubt that copper is less active than nickel.

It must be borne in mind, however, that the specific activities are based on surface areas as determined by argon adsorption at -196 ^{o}C, and if, as has been suggested by Tamaru [23] only a fraction of the superficial area of copper is in fact active, then the observed difference between the activities of copper and nickel would be considerably diminished. Duell and Robertson [68] found copper was more active than nickel for the decomposition of formic acid but these experiments were carried out at low pressures and conform to first order kinetics and so cannot be justifiably compared with the present results.

According to Bond [69], if there is no inhibition by the products of the decomposition as the reaction proceeds in a static system, the zero order reaction should change through a fractional order to first order with decrease in surface coverage by the reactant.

If plots of pressure increase against time are made for two runs at the same temperature but different initial pressures, in such a way that the partial pressure of formic acid in the reaction vessel is the same for any given point on the time axis, then the same deviation from zero order should be observed from both.

GRAPH 23

FORMIC ACID

Catalyst XV Temperature 190°C

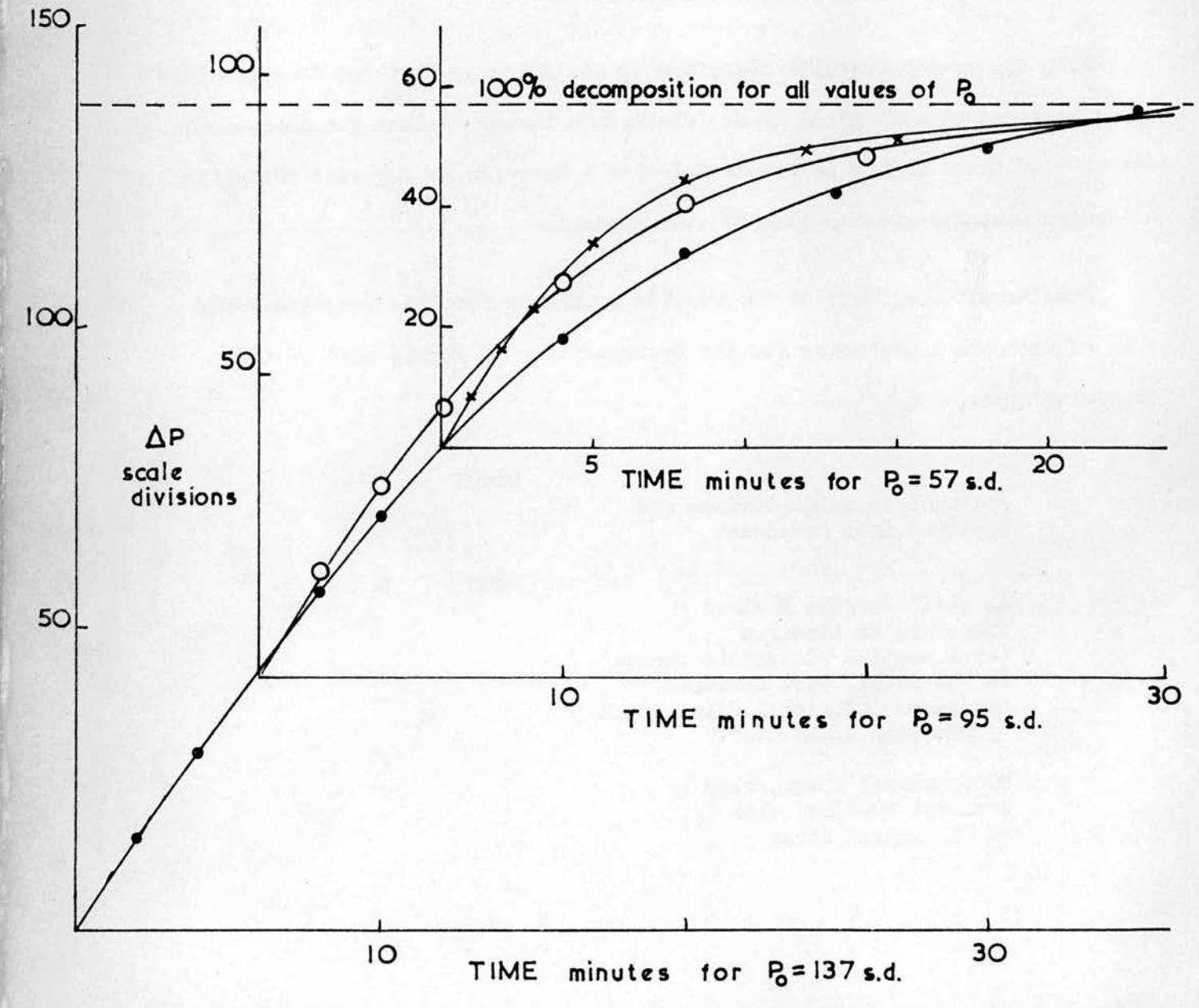

However if theproducts of the reaction have an inhibiting effect then the plots obtained will not be coincident since the rate controlling factor is no longer the fractional coverage of the surface by adsorbed formic acid.

Such plots are shown in Graph 23 for the decomposition of three different initial pressures of formic acid on Catalyst XV at 190 °C. They show a considerable difference in reaction rate (ie. slope) for the same partial pressure of formic acid which indicates that the products of the decomposition have an inhibiting effect on the reaction rate.

From the present results therefore it would appear that thé decomposition is to some extent controlled by an 'electronic factor ' since the decrease in activity of these alloys is associated with a decrease in magnetic susceptibility at copper contents greater than 80 atom percent.

Consideration of many of the results available for this reaction would seem to indicate a mechanism for the decomposition of formic acid of the following type.,

Approach to metal surface and break up into radicals.

At metal surface H atom transfers an electron (or a partial electronic change) to the metal, c.f. decrease in resistance of nickel films found by Suhrmann and Wedler.

HCOO radical chemisorbed by covalent bonding, with δ^- on the oxygen atoms.

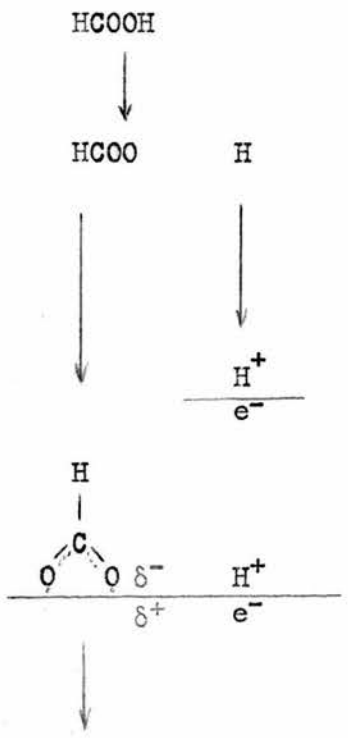

Loss of H from covalently adsorbed 'formate' and charge transfer back to the surface. Electron transfer back to H^+ from surface.

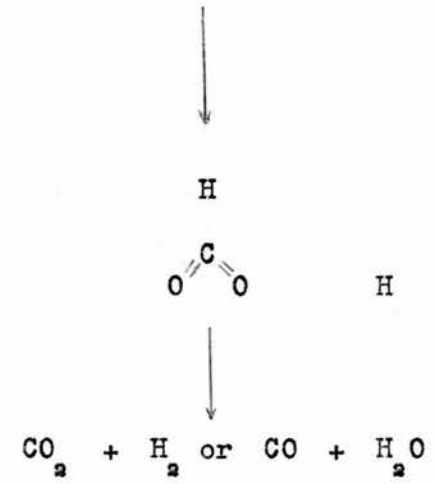

Combination of H with H or O and desorption of products.

$$CO_2 + H_2 \text{ or } CO + H_2O$$

In the proposed mechanism the breaking down of the activated complex and desorption of the products will probably be the rate determining factors [6]. It was in fact observed during the present work when HCOOH was first admitted to the catalyst that adsorption on nickel was fast and on copper it was noticably slower. This is to be expected from the above mechanism where the initial stages involve transfer and sharing of electronic charge with the metal, nickel having a greater concentration of vacant electronic states than copper.

The 'formate' radical, (to be in keeping with many of the results in the literature) will probably be essentially covalently bound rather than involve an electron transfer from the metal to produce an ion. The breaking of the complex and desorption of the products involves the transfer of electronic charge back to the hydrogen ion from the metal and the breaking of the C - H bond. The hydrogen atoms then combine (not necessarily intramolecularly) to produce molecular hydrogen.

From the results of Tamaru [23] it appears that the desorption of carbon dioxide is slower than that of hydrogen, on nickel four times as much formic acid had to be adsorbed in the initial stages for the evolution of carbon dioxide as for the evolution of hydrogen.

On copper the reaction rate was independent, but the degree of adsorption dependent, on the formic acid pressure, indicating that only part of the surface was active, and that the rate determining steps involve the desorption of products. The desorption of hydrogen, on the basis of the mechanism proposed above, involves the transfer of an electron from the metal and, from the results of Tamaru [23], is believed not to be rate determining. Hydrogen desorption will tend to lower the Fermi level and thus strain the covalently bound'formate' causing it to break up with the desorption of carbon dioxide. The breakdown of $(HCOO)^{\delta-}$ with charge transfer to the metal will be accentuated in nickel and alloys where d-band vacancies exist, since the Fermi level in these cases will be lower than in pure copper. Therefore nickel and these alloys should show greater activity than copper.

The existance of both carbon monoxide and carbon dioxide in the products are not explained by this mechanism. In many cases the reported yields of carbon monoxide can be accounted for by the catalyst support but the high yields found with nickel films by Walton and Verhoek [48] and in the flow system mentioned in this work [50] cannot be ascribed to this. The presence of traces of water in the formic acid or of a slight oxide layer on the catalyst may account for the large quantities found, or it may be that both gases are formed on dissociation of the activated complex, and the varying quantities reported in the literature are dependent on the analytical procedure. Rapid cooling and analysis of the desorbed gases is desirable so that any obscuring of the true decomposition products by a water gas shift is eliminated.

The Dutch workers have rejected any part which an electronic factor may play in the catalytic decomposition and have related the activities of the metals to the heat of formation of their formates [20,21,66].

By plotting the heat of formation of the metal formates against the temperature at which formic acid decomposes at a fixed rate (0.16 molecules site $^{-1}$ sec.$^{-1}$) on these metals, a 'volcano shaped' curve was obtained. This they claim to be in agreement with that qualitatively suggested by Balandin [70]. The activation energy (23 $\pm$ 2 kcal. mole^{-1}) and pre-exponential factor (log A = 9.8 $\pm$ 1.0) for the decomposition of formic acid on silica supported nickel given by Fahrenfort and Sachtler, are in agreement with those found in this present work, within experimental error, (24.2 $\pm$ 0.6 kcal. mole $^{-1}$ and log A = 10.6 where A is measured in molecules site $^{-1}$ sec. $^{-1}$) They have not investigated the decomposition on copper but have used the results of Tamaru [23] who carried out the decomposition between 65 and 100 ^{o}C (and not between 165 and 200 ^{o}C as stated by Fahrenfort and Sachtler). Extrapolation of the reaction rate (which they stated they avoided) was therefore carried out over 60 ^{o}C.

Extrapolation of some of the results in the literature to give a reaction rate of 0.16 molecules site $^{-1}$ sec. $^{-1}$ for the decomposition on copper has been carried out. The temperatures at which this rate was reached are summarised in the following table.

Temperature Range Studied ^{o}C	Temperature ^{o}C at which Rate = 0.16 mols. site^{-1} sec.$^{-1}$	Reference
65 - 100	158	Tamaru [23]
	214	Schwab [17]
250 - 300	240	Dowden and Reynolds [9]
150 - 200	302	XV This work
110 - 170	205	XVA This work

Summarising on the same basis as the Dutch workers, the result of Dowden and Reynolds should be most suitable for inclusion in their 'volcano shaped' curve, but the temperature obtained from this result is more than 80 °C too high to fit into the curve. All the other results give temperatures in excess of that required by this theory.

The decomposition of cupric formate has been reported by Keller and Korosy [71] as taking place via the formation of a volatile cuprous formate which subsequently decomposes to metallic copper leaving a film of copper on the wall of the reaction vessel. No such film has been reported in the literature cited in the table above, nor was it detected in the present work, which suggests that no volatile copper intermediate is produced.

It is clear therefore that the formate ion interpretation is not without its failings as also is its strongly criticised counterpart, the electronic factor. From the present results it would seem that the electronic factor plays a part in this decomposition but its effect may be obscured by many complicating factors.

The methanol decomposition as a test reaction on metals has not received as much attention as the formic acid reaction. This is probably due to the kinetics of the reaction being more complicated.

The predominant process when methanol decomposes on metals is dehydrogenation to carbon monoxide and hydrogen although on some selective catalysts formaldehyde is produced. Frackiewicz [72] has shown on thermodynamic grounds that carbon monoxide and hydrogen will be the main products of the decomposition between 250 and 450 °C.

The decomposition has been reported by Brihta and Luetic [73] to be zero order on a Raney copper catalyst between 150 and 250 °C, while Darby and Kemball [74] have shown it to conform to the following rate expression,

$$\frac{-dP_M}{dt} = \frac{k\,P_M}{1 + bP_{CO}}$$

on a Fischer-Tropsch cobalt catalyst. Balandin and Teteni [27] have given a general equation for the catalytic dehydrogenation of alcohols derived from Balandin's general kinetic equation for unimolecular heterogeneous catalytic reactions in flow systems.

The results of the present work have been shown to conform to a rate expression of a similar type to that used by Darby and Kemball but as has already been pointed out the linear plot obtained could conform to any one of four expressions deduced from the Langmuir adsorption isotherm. The resulting arbitrary values of rate constants for the decomposition are therefore based on the assumption that k_M, k_P etc. are constant and so no great stress can be laid on the resulting activation energies. Furthermore, the latter could not be corrected for heats of adsorption. A more complete study of this system with respect to the retardation of the reaction by products will be necessary before any direct conclusions can be drawn from this approach. It seems likely that this retardation, however, is due to the strong adsorption of carbon monoxide which Darby and Kemball reported on the Fischer-Tropsch catalyst and which Bond [69] has concluded is pronounced on copper and nickel. Bond has also concluded that inhibition due to strong adsorption of hydrogen is unlikely.

The initial rate of the reaction for 2.5 percent decomposition was used to obtain a measure of the activation energy and activity for the decomposition over the series of copper-nickel alloy catalysts. The activation energies obtained in this manner did not show any great variation with composition (Graph 18). A somewhat similar pattern was apparent from the activation energies obtained from the 'Langmuir constants', the only exception being the very low activation energy obtained for the decomposition on the second preparation of the pure copper catalyst (XVA). The reason for this is not apparent. It is significant that these activation energies have values some 10 - 12 kcals. mole $^{-1}$ greater than those obtained from the initial rates of reaction. While no great significance can be attached to the precise value of the difference between the two sets of activation energies, the higher values are probably a consequence of the inhibiting effect of carbon monoxide an effect which does not appear in calculations based on initial rates.

The activation energy - composition pattern for the dehydrogenation of ethanol over alumina supported copper-nickel alloys reported by Brihta and Luetic is slightly different. It shows a constant activation energy for alloys up to 60 atom percent nickel and a slight increase with alloys of nickel content greater than 60 atom percent. No activity pattern or pre-exponential factors were given.

Dowden and Reynolds [9] have shown that the activity of alloys of copper and nickel for the decomposition of methanol decreases almost continuously with increasing copper content above approximately 30 atom percent copper, which decrease they attributed to an electronic factor.

The activity pattern obtained from the present work although quite different to that of Dowden and Reynolds also agrees with the electronic factor theory. This pattern (Graph 19) is similar to that given in figure C on page 62 which is what would be expected from the copper-nickel system where d-band vacancies exist at copper contents above the critical composition. This pattern is of the same type as that found for the formic acid decomposition on these alloys but it is more pronounced, a much greater decrease in activity being apparent at high copper contents.

The valency bond theory of Pauling [5] has been adapted by Hall and Emmett [10] to the alloys of copper and nickel. For the hydrogenation of ethylene they have made plots showing the dependence of activity on the percentage d-character, on valency, and on the product of both of these functions. On this basis plots were made for the methanol decomposition. They are shown in Graph 21. The activity patterns obtained in this way show the same characteristics as the pattern in Graph 19 where the activity was plotted against alloy composition, and so no new feature is obtained from this approach.

A further indication of the loss of activity at high copper content is given in Graph 20. A compensation effect is apparent for all the catalysts except the alloy containing 92.6 atom percent copper and the pure copper catalyst. For the latter catalysts the loss of activity is not due to any great increase in activation energy but to a decrease in the pre-exponential factor. As suggested by Tamaru [23] for the formic acid decomposition, this could be due to only a fraction of the superficial area of copper being active, thus obscuring any effect which the electronic factor may have on the decomposition.

Since similar activity patterns for the decomposition of methanol and of formic acid on these alloys of copper and nickel were obtained, it seems likely that the decompositions are controlled by the same or similar factor. On the basis of the proposed formic acid mechanism it therefore appears that the methanol decomposition takes place via a chemisorbed complex of a type similar to that given below.

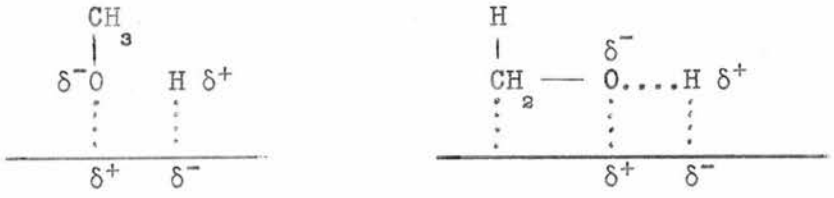

This type of complex is in keeping with the observations of Anderson and Kemball [75] who, for deuterium exchange reactions of alcohols on various metal catalysts, found that exchange took place much more easily with the hydroxyl hydrogen than with hydrogen in the methyl group.

The mechanism proposed by Balandin [27] and substantiated by Luetic and Brihta [76] involved a complex of the following type.

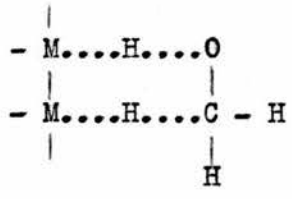

This is in keeping with their claims that two hydrogen atoms are removed simultaneously from the alcohol to the catalyst. Luetic and Brihta report that copper is a better catalyst than nickel for the dehydrogenation of alcohols. This they base on the lower values of activation energy found for copper.

No attempt was made to obtain a pre-expenential factor or a specific activity for these results. This is in direct disagreement with the present results and indeed with the electronic factor concept, but, as has been pointed out by many workers, results based entirely on activation energy values often give an incorrect picture.

Among the many complicating factors in the formic acid decomposition, may be mentioned the water gas shift commented on by Fahrenfort and Sachtler [20], and the marked inhibition of the reaction which appears after roughly half of the formic acid has decomposed by a zero order process and to which the term 'inhibited zero order' has been applied. Future work will clearly require a classical study of the kinetics of the reaction to determine the influence of hydrogen, carbon monoxide and carbon dioxide on the rate (to supplement the results of Walton and Verhoek [48]), and also measurement of the CO / CO_2 ratio during the entire course of the reaction and particularly in the initial zero order stage.

As in the formic acid reaction a 'classical' study of the kinetics of the methanol decomposition on these alloys is desirable to investigate the influence of the products of the reaction on the reaction rate. Infra-red studies of the surface during chemisorption as have been carried out in investigations of the formic acid reaction, and examination of the decomposition products of various deuterated methanols, would also help to elucidate many aspects of the decomposition.

From this study it is clear that the copper-nickel system is not a completely satisfactory one for the study of an electronic factor in catalysis. In spite of this however, as far as can be ascertained, both test reactions investigated show a dependency on the electronic structure of the catalyst.

REFERENCES

1. Dowden, D.A., J. Chem. Soc., (1950) 242.

2. Roginskii, S. and Schul'tz, E., Z. physik. Chem. A138 (1928) 21.

3. Baker, M. and Jenkins, G.I., Advances in Catalysis VII (1955) 1.

4. Griffith, R.H., 'Advances in Catalysis and Related Subjects' Vol. 1 New York Academic Press, 1948.

5. Pauling, L., Proc.Roy. Soc. A196 (1949) 343.

6. Mott, N. and Jones, H., 'Properties of Metals and Alloys' O.U.P. London.

7. Owen, E.A. and Pickup, B., Z. Krist. 88 (1934) 116.

8. Bond, G.C. and Mann, R.S., J. Chem. Soc., (1959) 3566.

9. Dowden, D.A. and Reynolds, P.W., Disc. Faraday Soc., 8 (1950) 184.

10. Hall, W.K. and Emmett, P.H., J. Phys. Chem., 63 (1959) 1102.

11. Best, R.J. and Russell, W.W., J. Amer. Chem. Soc. 76 (1954) 838.

12. Hall, W.K. and Emmett, P.H., J. Phys. Chem. 62 (1958) 816.

13. Rienacker, G. and Bommer, E.A., Z. anorg. Chem. 242 (1939) 302.

14. Tuul, J. and Farnsworth, H.E., J. Amer. Chem. Soc., 83 (1961) 2247.

15. Rienacker, G. and Bade, H., Z. anorg. Chem. 248 (1941) 45.

16. Luetic, P.F. and Brihta, I., Croat. Chim. Acta, 31 (1959) 75.

17. Schwab, G.M. and Schwab-Agallidis, Ber. 76 (1943) 1228.

18. Eley, D.D. and Luetic, P., Trans. Faraday Soc. 53 (1957) 1483.

19. Schwab, G.M., Trans. Faraday Soc. 42 (1946) 689.

20. Fahrenfort, J., van Reyen, L. and Sachtler, W.M., 'The Mechanism of Heterogeneous Catalysis' de Boer, J.M., Elsevier Monograph, 1960.

21. Fahrenfort, J. and Sachtler, W.M., Proc. 2nd International Congress on Catalysis, Editions Technip, Paris, 1961, 1 831.

22. Hirota, K., Kuwata, K. and Nakai, Y., Bull. Chem. Soc. Japan, 31 (1958) 861.

23. Tamaru, K., Trans. Faraday Soc., 55 (1959) 824 and 1191.

24. Suhrmann, R. and Wedler, G., 'Advances in Catalysis' IX (1956) 223.

25. Ruka, R.J., Blockway, L.O. and Boggs, J., J. Amer. Chem. Soc. 81 (1959) 2930.

26. Constable, F.H., Proc. Roy. Soc. (London) A108 (1925) 355.

27. Balandin, A. and Teteni, P., Zhur. fiz. Khim. 35 (1961) 62.

28. Gharpurey, P. and Emmett, P.H., J. Phys. Chem. 65 (1961) 1182.

29. Long, J., Frazer, J. and Ott, E., J. Amer.Chem. Soc. 56 (1934) 1101.

30. Hall, W.K. and Alexander, L., J. Phys. Chem. 61 (1957) 242.

31. Brunauer, S., Emmett, P.H. and Teller, E., J. Amer. Chem. Soc. 60 (1938) 309.

32. Schriener, F. and Kemball, C., Trans. Faraday Soc., 49 (1953) 190.

33. Huttig, G., Monatsh. Chem., 78 (1948) 177.

34. Farkas and Melville, 'Experimental Methods in Gas Reactions' McMillan (London) 1939, p.104.

35. Coles, B.R., J. Inst. Metals, 84 (1956) 346.

36. Coles, B.R., Proc. Phys. Soc. 65B (1952) 221.

37. Figgis, B. and Nyholm, R., J. Chem. Soc. (1958) 4190.

38. Pugh, E.W. and Ryan, F.M., Phys. Rev. 111 (1958) 1038.

39. Pugh, E. W., Ryan, F.M. and Smoluchowski, R., Phys. Rev. 116 (1959) 1106.

40. Kaufmann, A.D. and Starr, C., Phys. Rev. 63 (1943) 445.

41. Reynolds, P.W., J. Chem. Soc. (1950) 265.

42. Lewis and Wilkins , 'Modern Coordination Chemistry' Interscience Publishers New York , 1960.

43. Coolidge, A.S., J. Amer. Chem. Soc. 52 (1930) 1874.

44. Ewins, A.J., J. Chem. Soc. 105 (1914) 354.

45. Blake, P.G. and Hinshelwood, C., Proc. Roy. Soc. A255 (1960) 444.

46. Coolidge, A.S., J. Amer. Chem. Soc. 50 (1928) 2166.

47. Ramsperger, H. and Porter, C., ibid 3036.

48. Walton,D.K. and Verhoek, F.H., 'Advances in Catalysis' IX (1956) 682.

49. Minchin, L.J., Ind. Chemist 30 (1954) 381.

50. Musgrave, R., Quinn, D. and Taylor, D., unpublished results.

51. Darby, P.W. and Kemball, C., Trans. Faraday Soc. 53 (1957) 832.

52. Alder, M., Thesis, Zurich, 1916.

53. Ahern, S.A., Martin, M. and Sucksmith, W., Proc. Roy. Soc. A248 (1958) 145.

54. Wohlfarth, W., Proc. Roy. Soc. A195 (1949) 434.

55. Weiss, R. and de Marco, J., Rev. Mod. Phys., 30 (1958) 59.

56. Svensson, B., Ann. Phys., Lpz. 14 (1932) 669.

57. Sabatka, J. and Selwood, P.W., J. Phys. Chem., 61 (1957) 1564.

58. Rienacker, G. and Burmann, R., J. prakt. Chem. 158 (1941) 95.

59. Rienacker, G. and Unger, S., Z. anorg. Chem. 274 (1953) 47.

60. Rienacker, G. and Vormum, G., Z. anorg. Chem. 283 (1956) 287.

61. Shallcross, P. and Russell, W.W., J. Amer. Chem. Soc. 81 (1959) 4132.

62. Schwab, G.M., Disc. Faraday Soc. 8 (1950) 166.

63. Rienacker,G. and Hansen, N., Z. anorg. Chem. 284 (1956) 162.

64. Rienacker, G. and Hansen, N., Z. Elektrochem. 60 (1956) 887.

65. Suhrmann, R. and Wedler, G., Z. Elektrochem. 60 (1956) 892.

66. Fahrenfort, J., van Reyen, L. and Sachtler, W., Z. Elektrochem. 64 (1960) 216.

67. Eishens, R. and Pliskin, W., Proc. 2nd International Congress on Catalysis, (Editions Technip, Paris, 1961) 1 789.

68. Duell, R. and Robertson, A.J., Trans. Faraday Soc. 57 (1961) 1416.

69. Bond, G. , 'Catalysis by Metals' Academic Press, (1962).

70. Balandin, A., Zuhr. fiz. Khim., 31 (1957) 745.

71. Keller, A. and Korosy, F., Nature, 162 (1948) 580.

72. Frackiewicz, C., Premysl Chem. 39 (1960) 752.

73. Brihta, I. and Luetic,P.F., Croat. Chim. Acta, 28 (1956) 93.

74. Darby, P.W. and Kemball, C., Trans. Faraday Soc. 53 (1957) 832.

75. Anderson, J. and Kemball, C., Trans. Faraday Soc. 51 (1955) 966.

76. Brihta, I. and Luetic, P.F., Croat. Chim. Acta, 29 (1957) 419.